

Final Report

The Installation, Operation and Analysis of Eddy Covariance for Quantifying Evapotranspiration

April 1st, 2024



S. Tyson McKinney¹, Michael H. Young¹

¹Bureau of Economic Geology, Jackson School of Geosciences, The University of Texas at Austin,
Austin, Texas 78758, USA; Corresponding author: tyson.mckinney@beg.utexas.edu

Submitted to:
The Edwards Aquifer Authority, San Antonio, TX

EAA Contract No. 20-041-AMS

Table of Contents

Executive Summary	4
1 Introduction.....	7
2 Site Installation and Maintenance	7
2.1 Site Overview	7
2.2 Cibolo (US-EA4).....	9
2.3 Uvalde (US-EA5).....	12
2.4 Nueces (US-EA6).....	13
3 Data Processing.....	16
3.1 Overview	16
3.2 EasyFlux-DL Processing (<i>Raw Data</i> → <i>Half-Hourly Data</i>)	18
3.3 BEG QA/QC (<i>Half-Hourly Data</i> → <i>BEG Filtered Data</i>)	19
3.3.1 Formatting and Converting Units	19
3.3.2 Backfilling SW_IN at Cibolo (US-EA4) and SW_IN and P at Uvalde (US-EA5)	20
3.3.3 Filtering.....	23
3.4 BEG Processing (<i>BEG Filtered Data</i> → <i>Provisional ET Data</i>).....	26
3.4.1 Gap-Filling.....	26
3.4.2 ET Calculation and Bowen-Correction of LE and H.....	26
3.4.3 <i>Provisional ET Data</i> Product.....	27
3.5 AmeriFlux QA/QC & Processing	30
3.5.1 Overview.....	30
3.5.2 AmeriFlux QA/QC (<i>BEG Filtered Data</i> → <i>BASE Product</i>).....	30
3.5.3 AmeriFlux ONEFlux Processing (<i>BASE Product</i> → <i>FLUXNET Product</i>).....	30
4 Results and Discussion	31
4.1 Data Processing.....	31
4.1.1 Cibolo Site (US-EA4).....	32
4.1.2 Uvalde Site (US-EA5)	33
4.1.3 Nueces Site (US-EA6).....	34
4.1.4 Summary of Results of Processing Steps.....	34
4.2 Limitations of Processed Data.....	44
4.3 Preliminary Water Budget Analysis.....	47
4.3.1 Cumulative P and ET used in Water Budget Analyses.....	47
4.3.2 Monthly P and ET.....	49
5 Recommendations for Future Work.....	53
5.1 Maintenance and Operation	53
5.2 Data Processing	54
5.3 Water Budget Analyses.....	54
References.....	54

List of Figures

Figure 2.1 Site Map.....	8
Figure 2.2 Field Photographs of Cibolo (US-EA4) Site.....	9
Figure 2.3 Field Photographs of Cibolo (US-EA4) Station Maintenance.	11
Figure 2.4. Field Photographs of Uvalde (US-EA5) Station.	12
Figure 2.5. Photographs of Nueces (US-EA6) Station Installation.	14
Figure 2.6. Field Photographs of Nueces (US-EA6) Site.	15
Figure 2.7. Field Photographs of Nueces (US-EA6) Station Maintenance.	15
Figure 3.1. Eddy Covariance Data QA/QC and Processing Flowchart.	17
Figure 3.2. Comparison of SW_IN at Cibolo and BEX01WS.	21
Figure 3.3. Comparison of SWC Measured at Uvalde Site and EAA Weather Station.	22
Figure 4.1. Percentage of Missing Data for Cibolo Throughout QA/QC and Processing.....	32
Figure 4.2. Percentage of Missing Data for Uvalde Throughout QA/QC and Processing.	33
Figure 4.3. Percentage of Missing Data for Nueces Throughout QA/QC and Processing.....	34
Figure 4.4. Timeseries of LE Data for Cibolo at Each QA/QC and Processing Step.....	36
Figure 4.5. Subset of LE Data for Cibolo at Each QA/QC and Processing Step.....	37
Figure 4.6. Timeseries of LE Data for Uvalde at Each QA/QC and Processing Step.....	38
Figure 4.7. Subset of LE Data for Uvalde at Each QA/QC and Processing Step.....	39
Figure 4.8. Timeseries of LE Data for Nueces at Each QA/QC and Processing Step.....	40
Figure 4.9. Subset of LE Data for Nueces at Each QA/QC and Processing Step.....	41
Figure 4.10. Comparison of Cumulative ET at Cibolo After Each QA/QC Processing Step.....	42
Figure 4.11. Comparison of Cumulative ET at Uvalde After Each QA/QC Processing Step.....	43
Figure 4.12. Comparison of Cumulative ET at Nueces After Each QA/QC Processing Step.....	44
Figure 4.13. Original and Reprocessed Half-Hourly Data at Cibolo from Jan-Apr 2023.....	46
Figure 4.14. Original and Reprocessed Half-Hourly Data at Cibolo from Jul-Oct 2023.	47
Figure 4.15. Cumulative P and ET at the Cibolo Site.....	48
Figure 4.16. Cumulative P and ET at the Uvalde Site.....	49
Figure 4.17. Cumulative P and ET at the Nueces Site.....	49
Figure 4.18. Monthly Water Budget at the Cibolo Site.....	50
Figure 4.19. Monthly Water Budget at the Uvalde Site.	51
Figure 4.20. Monthly Water Budget at the Nueces Site.....	52

List of Tables

Table 2.1 Eddy Covariance Station Metadata.....	8
Table 2.2 Cibolo (US-EA4) Maintenance History	11
Table 2.3 Uvalde (US-EA5) Maintenance History.....	13
Table 2.4 Nueces (US-EA6) Maintenance History.....	16
Table 3.1. Physical and Expected Limits for AmeriFlux Variables	24
Table 3.2 <i>Provisional ET Data</i> Variable Metadata	29
Table 4.1. Amount of Missing Flux Measurements for Cibolo During QA/QC Steps	32
Table 4.2. Amount of Missing Flux Measurements for Uvalde During QA/QC Steps.....	33
Table 4.3. Amount of Missing Flux Measurements for Nueces During QA/QC Steps.....	34
Table 4.4. Cumulative P – ET Values Calculated for Water Years [mm].....	48
Table 4.5. Monthly Water Budget for Cibolo (US-EA4)	50
Table 4.6. Monthly Water Budget for Uvalde (US-EA5).....	51
Table 4.7. Monthly Water Budget for Nueces (US-EA6)	52

Executive Summary

During the contract period from January 2021 through December 31, 2023, the University of Texas at Austin, Bureau of Economic Geology (UT-BEG) installed and maintained two eddy covariance stations across the Edwards Aquifer recharge region. The Cibolo station was installed on February 25, 2021, in the more humid eastern portion of the region within an oak-ashe juniper ecosystem adjacent to Cibolo Creek at the Field Research Park (FRP) operated by the Edwards Aquifer Authority (EAA). The Uvalde station was installed on April 8, 2021, in the more arid western portion of the region within a mesquite woody savanna northwest of Uvalde, TX, near the Nueces River. The Uvalde station was demobilized on March 1, 2023, and relocated to a permanent location approximately 30 miles north, within an oak-ashe juniper woody savanna on the Shield Ranch east of Camp Wood, TX, and renamed the Nueces station. Installation of the Nueces station was completed on July 19, 2023. Site visits were performed throughout the contract period for regular maintenance, such as calibrating (i.e., zero-spanning) the infrared gas analyzer, and as-needed maintenance such as troubleshooting issues with power, communication or individual sensors. The Cibolo, Uvalde, and Nueces sites have been registered with AmeriFlux (a collaborative network of flux site across North, Central, and South America with standardized processes and procedures) with site designations of US-EA4, US-EA5, and US-EA6, respectively. Data submission to AmeriFlux for the eddy covariance sites is ongoing.

A thorough data processing pipeline was established to ensure high quality data and includes steps performed (1) on-site by the manufacturer (Campbell Scientific), (2) within UT-BEG offices, and (3) at the AmeriFlux facility. Each station collects high frequency (10-Hz) measurements of three-dimensional wind speed and direction, and concentrations of carbon dioxide (CO₂) and water vapor; and, low frequency (5-minute) measurements of meteorological parameters (e.g., soil heat flux, water content and temperature, pressure, relative humidity, etc.), all of which are processed using a program installed on the datalogger to produce data at half-hourly intervals (*Half Hourly Data*). Quality assessment and quality control (QA/QC) measures are performed on the *Half-Hourly Data* by UT-BEG, such as inspecting variable format, sign conventions, and units; filtering data based on QC grades and the number of 10-Hz measurements in a half-hour period; and identifying and removing statistical outliers. The UT-BEG QA/QC'd dataset (*BEG Filtered Data*) is further processed by UT-BEG to gap-fill flux data and calculate

evapotranspiration (ET) before and after a Bowen correction is applied (*Provisional ET Data*). The *BEG Filtered Data* are concurrently sent to AmeriFlux for further QA/QC (*BASE Product*) and processing (*FLUXNET Product*), such as gap-filling and calculation of meteorological parameters, including ET and net ecosystem exchange. Once processed, the *BASE Product* and *FLUXNET Product* are posted to the AmeriFlux website and made available to the scientific community. Moving forward, the *Provisional ET Data* product will be sent to EAA on a quarterly basis. The *FLUXNET Product* will be sent to EAA on an annual, or 6-month, basis, and will be considered final. Data processing applied by UT-BEG results in removal of up to ~40% of latent heat flux (LE) data, from which ET is directly calculated. Gap-filling procedures fill in the majority of these missing data, although gaps still exist where similar meteorological conditions are not available for gap-filling and/or when longer gaps were generated due to sensor failure or a lack of power supplied to the station.

Preliminary water budget analyses were performed at each site at monthly and “water year” time scales, with water years beginning on October 1 and ending on September 30 of the following year and named for the year in which they end. The Cibolo site showed the potential for recharge (i.e., precipitation [P] exceeds ET) in water years 2021, 2023, and 2024 with P exceeding ET by 110 mm, 33 mm, and 81 mm, respectively. A deficit (i.e., ET exceeded P) of 15 mm occurred in water year 2022, although a six-week gap in data collection exists when the station was without power. The Uvalde site experienced a deficit in water year 2021 of 28 mm, but an excess of P in water years 2022 and 2023 of 84 mm and 40 mm, respectively. So far in water year 2024 (as of December 31, 2023) at the Nueces site, P has exceeded ET by 65 mm. At a monthly timescale, P generally equaled or exceeded ET at all three sites during spring, fall and winter months, indicating a potential for recharge during those seasons. During the summer months, ET generally exceeded P at all three sites. These preliminary water budget analyses ignore changes in storage (i.e., soil and rock water content) and runoff, each of which likely contribute to the overall potential for recharge across the region. Future water budget analyses will need to consider these components, as well as the frequency and intensity of individual precipitation events and the “memory” of the system (i.e., near-term differences in monthly P and ET may have a larger or smaller impact on recharge, depending on past wet and dry periods). Future work will also focus on upscaling the results by correlating direct measurements of ET at the eddy covariance stations to remotely-

sensed datasets, such as vegetation indices (e.g., EVI and NDVI) or solar-induced fluorescence (SIF), and model-based regional ET datasets, such as OpenET.

1 Introduction

The need to understand groundwater recharge and other water balance components in the Edwards Aquifer region are substantial and ongoing given future climate variability and increased population, which will further stress the supply and demand of regional water resources (Sharp et al., 2020; Loáiciga and Schofield, 2020). Climate, vegetation, and soils each exert controls on groundwater recharge to various extents and at different scales. Mean annual precipitation is estimated to explain 80% of the variation in recharge across Texas (Keese et al., 2005), but the incredible diversity of vegetation and climate in Texas makes local recharge estimates very difficult to assess. Evapotranspiration (ET) is a major component of any local water budget and the most difficult to quantify, further complicating recharge estimates.

In karst terrain, most recharge is focused directly from losing streams, while a smaller, less temporally dynamic proportion originates as diffuse recharge through the soil material between stream channels (Marclay, 1995; Wong et al., 2012), which is sometimes referred to as interfluvial recharge. A previous study by the University of Texas, Bureau of Economic Geology (UT-BEG) suggested that ~4% of total precipitation at Camp Bullis (just north of San Antonio) is being recharged through diffuse routes (Sun et al., 2020). That study used direct measurements of ET in three different vegetation domains within the same climate to estimate diffuse recharge. The eddy covariance systems used to measure ET in the Camp Bullis project were relocated to different locations to explore the control of climate on ET rates. One station was established in the more humid eastern portion and a second in the more arid western portion of the Edwards Aquifer recharge and contributing zones. Long-term data from these sites will help constrain the effects of climate variability on ET, and hence, diffuse recharge, and allow for more accurate upscaling of direct measurements across the entire recharge zone.

2 Site Installation and Maintenance

2.1 Site Overview

Three eddy covariance stations were installed, operated and maintained during this contract period, with two of the stations still in operation (Figure 2.1 and Table 2.1). Details on installation and maintenance of each station are provided in the following sections and additional information

can be found in the quarterly reports associated with this contract. All three sites have been registered with the AmeriFlux network and AmeriFlux site designations (US-EA_) are included with the site names throughout the remainder of this report.

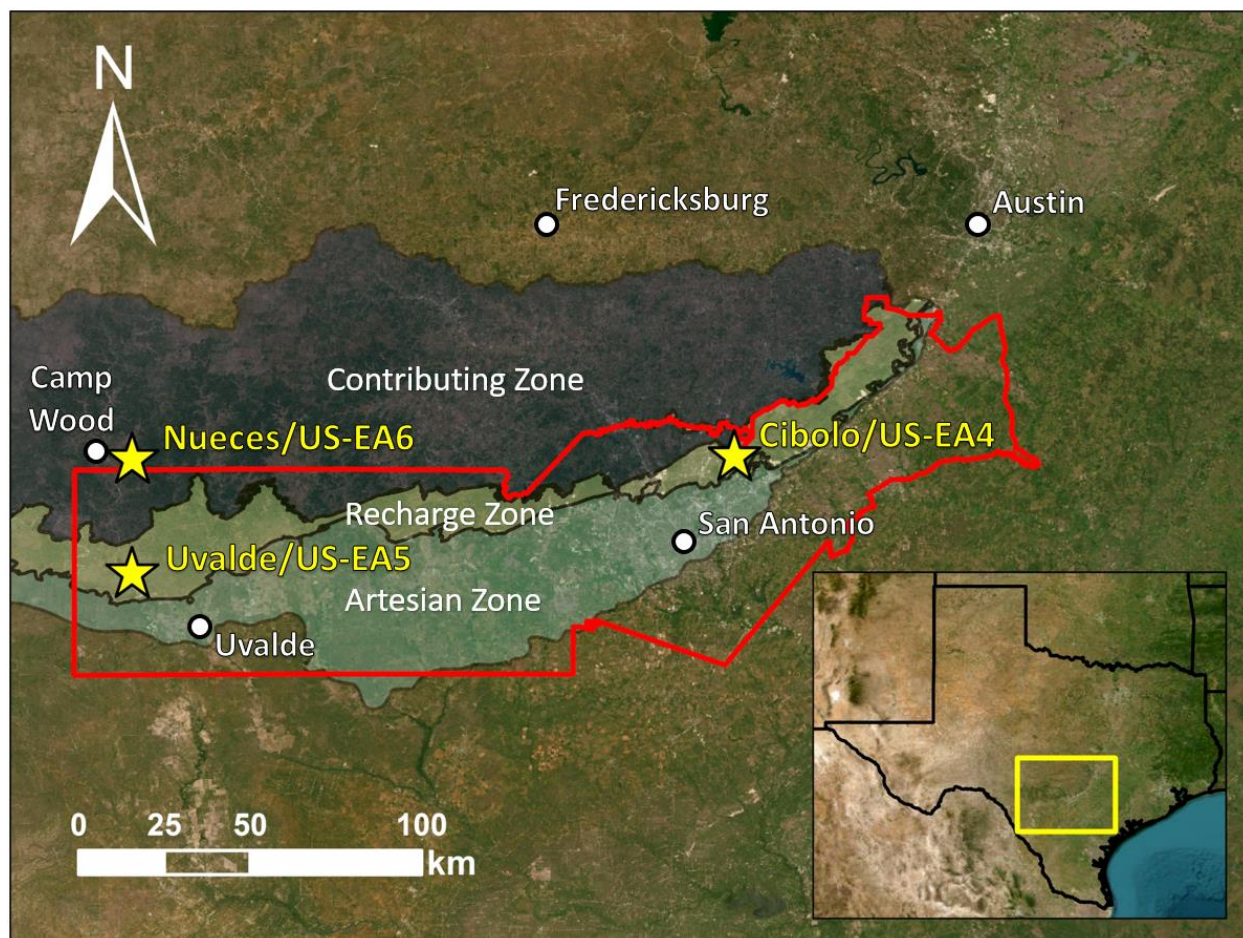


Figure 2.1 Site Map. Regional map showing the locations of the eddy covariance stations with respect to the Edwards Aquifer contributing, recharge, and artesian zones and the jurisdictional area of the EAA outlined in red (credit: EAA); inset shows location of regional map within the state of Texas.

Table 2.1 Eddy Covariance Station Metadata

Site Name	Cibolo	Uvalde	Nueces
AmeriFlux Site Code	US-EA4	US-EA5	US-EA6
Latitude	29.6633°	29.355° [†]	29.65611°
Longitude	-98.3817°	-99.954° [†]	-99.95878°
Elevation	297 m	322 m	480 m
Date of Installation	2/25/2021	4/8/2021	7/19/2023
Date of Removal	N/A	3/1/2023	N/A
Ecosystem	oak-ashe juniper woodland	mesquite woody savanna	oak-ashe juniper woody savanna

Canopy Height	8 m	4 m	7 m
Height of IRGASON	10.85 m	7.28 m	9.9 m
IRGASON Azimuth	156°	174°	160°

[†]Latitude and longitude are generalized and shown at reduced precision to protect privacy of landowner

2.2 Cibolo (US-EA4)

The first eddy covariance station was installed at the Edwards Aquifer Authority (EAA) Field Research Park (FRP) located near Cibolo Creek (henceforth referred to as the “Cibolo” site) in an oak-ashe juniper woodland ecosystem (Figure 2.2). The specific tower location was chosen based on a balance between enduring site access and minimizing variance in topography and vegetation characteristics (i.e., as flat and with as homogeneous of vegetation as possible). The tower was installed during the week of February 22, 2021, just after Winter Storm Uri. The site was initially prepared by EAA personnel, who secured and anchored permanent scaffolding 10 m in height, after which instrumentation was installed by UT-BEG personnel.



Figure 2.2 Field Photographs of Cibolo (US-EA4) Site. (left) Eddy covariance station at the Cibolo site; (right) drone photograph of Cibolo site looking into direction of sonic azimuth showing general characteristics of oak-ashe juniper ecosystem within measurement footprint.

The original installation of the station included a collocated infrared gas analyzer and 3-dimensional sonic anemometer (IRGASON, Campbell Scientific) and associated temperature probe and hardware (EC100, Campbell Scientific), a net radiometer (NRLite2, Kipp & Zonen), a tipping bucket rain gauge (TE525, Texas Electronics), and a set of ground-based sensors installed between 5-10 cm depth within a single pit that included two soil heat flux plates (HFP01, Hukseflux) and four soil water content, temperature and electrical conductivity sensors (CS655, Campbell Scientific). Data was collected using the EasyFlux-DL program installed on a CR3000 datalogger. In January 2023, the station was upgraded to maintain state of the art instrumentation and data collection. These upgrades included replacing the CR3000 datalogger with a CR1000X datalogger (and updated EasyFlux-DL program), and installing a 4-way radiometer (SN500SS, Apogee), a photosynthetically-active radiation (PAR) sensor (CS310, Apogee), and a second set of ground-based sensors in a secondary pit (Figure 2.3). The new set of ground-based sensors included one self-calibrating heat-flux plate (HFP01SC, Hukseflux), one soil water content, temperature and electrical conductivity sensor (CS655, Campbell Scientific) and one averaging soil thermocouple probe (TCAV, Campbell Scientific). The station is powered by a solar panel and 12V-80Ah battery and data are transmitted to UT-BEG using a cell modem (RV50, Sierra Wireless) and SIM card.

Maintenance of the station occurred on an as-needed basis and included troubleshooting power and/or communication issues, upgrading and maintaining instrumentation, and calibrating (i.e., performing a zero-span on) the IRGASON (Figure 2.3). All maintenance that occurred during the contract period is summarized in Table 2.2 and detailed in the quarterly reports. Moving forward, regular site visits will be performed at least twice a year to service the IRGASON (i.e., clean lenses, replace rain wicks, level and perform a zero-span), test and calibrate the rain gauge, clean radiometer lenses and re-level, and address any further issues. Additional site visits will be made on an as-needed basis.



Figure 2.3 Field Photographs of Cibolo (US-EA4) Station Maintenance. (left) UT-BEG personnel performing a zero-span on the Cibolo station IRGASON from a lift; (right) installation of ground-based sensors in soil pit #2 at the Cibolo site during the site upgrade in January 2023.

Table 2.2 Cibolo (US-EA4) Maintenance History

Date	Maintenance Performed
2/22/2021	Installation of Cibolo site
3/9/2022	Power-cycled datalogger to resume data collection and transmission
4/13/2022	Changed out desiccant; updated CR3000 datalogger OS to version 32.05; updated EasyFlux program to have “ManualOn” switch; swapped out memory card
5/20/2022	Performed a zero-span on IRGASON; changed out desiccant in EC100 control box; moved cellular antenna ~10’ higher on the scaffolding
10/4/2022	Cleaned IRGASON gas analyzer lenses with isopropyl alcohol to address issue with CO ₂ and H ₂ O signal strengths
1/12/2023 – 1/13/2023	Replaced CR3000 datalogger with CR1000X datalogger; installed new EasyFlux program; installed 4-way radiometer (SN500SS); installed PAR sensor (CS310); installed second set of ground-based sensors (one each of CS655, TCAV and HFP01SC) in a second soil pit
4/11/2023	Updated EasyFlux program to have a table to collect soil water content, temperature and electrical conductivity value from deeper soil sensors in soil pit #1; leveled 4-way radiometer and PAR sensor; installed bird spikes on radiometer mounting arms; cleaned IRGASON lenses, leveled IRGASON, replaced IRGA wicks (could not replace sonic wicks); installed bird spikes on IRGASON and mounting arm; performed a zero-span on IRGASON
5/17/2023	Re-installed all ground-based sensors in soil pit #1; deepened trench and ran ground-based sensor cables through conduit; changed SDI address of one of the “deep” soil sensors in soil pit #1 from 2 to 3; installed “Canopy PPT” stations ~20 m to the northwest of the EC

	tower (two TE525 tipping bucket rain gauges, one each under the dripline and denser canopy of a live oak tree)
7/25/2023	Changed out micro-SD card in datalogger; swapped out desiccant; leveled 4-way radiometer; re-installed rain gauge on inside of solar panel enclosure (was found to be on the ground with the funnel separated and bird spikes bent); tested rain gauge
12/13/2023	Updated EasyFlux-DL program to correct faulty line of code that was setting the “height_canopy” variable to a default value of 0.5 m; updated; changed out micro-SD card in datalogger

2.3 Uvalde (US-EA5)

The second eddy covariance station was installed on a trailer located on a private ranch approximately 20 km northwest of Uvalde, TX (henceforth referred to as the “Uvalde” site) within a relatively homogeneous mesquite woody savanna (Figure 2.4). The station was initially installed on March 29-30, 2021, and a return visit was performed on April 8, 2021, to finalize installation.



Figure 2.4. Field Photographs of Uvalde (US-EA5) Station. (left) Eddy covariance station at the Uvalde site; (right) photograph of the Uvalde site looking approximately into the direction of the sonic azimuth showing general characteristics of mesquite woody savanna ecosystem within measurement footprint (photograph taken in February 2023 during leaf-off conditions).

The Uvalde station included a collocated infrared gas analyzer and 3-dimensional sonic anemometer (IRGASON, Campbell Scientific) and associated temperature probe and hardware

(EC100, Campbell Scientific), a net radiometer (NRLite2, Kipp & Zonen), a tipping bucket rain gauge (TE525, Texas Electronics), and a set of ground-based sensors installed between 5-10 cm depth within in a single pit that included three soil heat flux plates (HFP01, Hukseflux), four soil water content, temperature and electrical conductivity sensors (CS655, Campbell Scientific) and an averaging soil thermocouple probe (TCAV, Campbell Scientific). Data were collected using the EasyFlux-DL program installed on a CR3000 datalogger and the station was powered by a solar panel and 12V-80Ah battery. Data were transmitted to UT-BEG using a cell modem (RV50, Sierra Wireless) and SIM card.

Due to changes in project personnel during the contract period and the decommissioning and relocation of the tower in March 2023, maintenance of the Uvalde station was limited. All maintenance that occurred during the contract period is summarized in Table 2.3 and detailed in the quarterly reports.

Table 2.3 Uvalde (US-EA5) Maintenance History

Date	Maintenance Performed
3/29/2021	Performed initial installation of station
4/8/2021	Finalized station installation (installed grounding rod, wiring, etc.)
9/21/2021	Performed maintenance on soil sensors
8/10/2022	Updated CR3000 datalogger OS to version 32.05; changed out memory card
3/1/2023	Decommissioned station

2.4 Nueces (US-EA6)

Due to a change in landowner access, the Uvalde station was decommissioned in March 2023 and relocated to a permanent site on the Shield Ranch approximately 5 km southeast of Camp Wood, TX (henceforth referred to as the “Nueces” site) and approximately 30 km north of the original Uvalde site. The station consists of a permanent tower located within an oak-ashe juniper woody savanna ecosystem and was initially installed on March 1, 2023. Several return visits were required to finalize installation, which was completed on July 19, 2023 (Figures 2.5 and 2.6).



Figure 2.5. Photographs of Nueces (US-EA6) Station Installation. (left) Installation of the tower structure for the Nueces site by EAA personnel; (right) installation of ground-based sensors by EAA personnel in pit #1 within a grass patch by the station solar panel.

The Nueces station includes a collocated infrared gas analyzer and 3-dimensional sonic anemometer (IRGASON, Campbell Scientific) and associated temperature probe and hardware (EC100, Campbell Scientific), a net radiometer (NRLite2, Kipp & Zonen), a 4-way radiometer (SN500SS, Apogee), a PAR sensor (CS310, Apogee), a tipping bucket rain gauge (TE525, Texas Electronics), and two sets of ground-based sensors installed between 5-10 cm depth in two separate pits. Each set of ground-based sensors includes one self-calibrating ground heat flux plate (HFP01SC, Hukseflux), one soil water content, temperature and electrical conductivity sensor (CS655, Campbell Scientific) and one averaging soil thermocouple probe (TCAV, Campbell Scientific). Data are collected using the EasyFlux-DL program installed on a CR1000X datalogger and the station is powered by a solar panel and 12V-80Ah battery. Data is transmitted to BEG using a cell modem (RV50, Sierra Wireless) and SIM card.

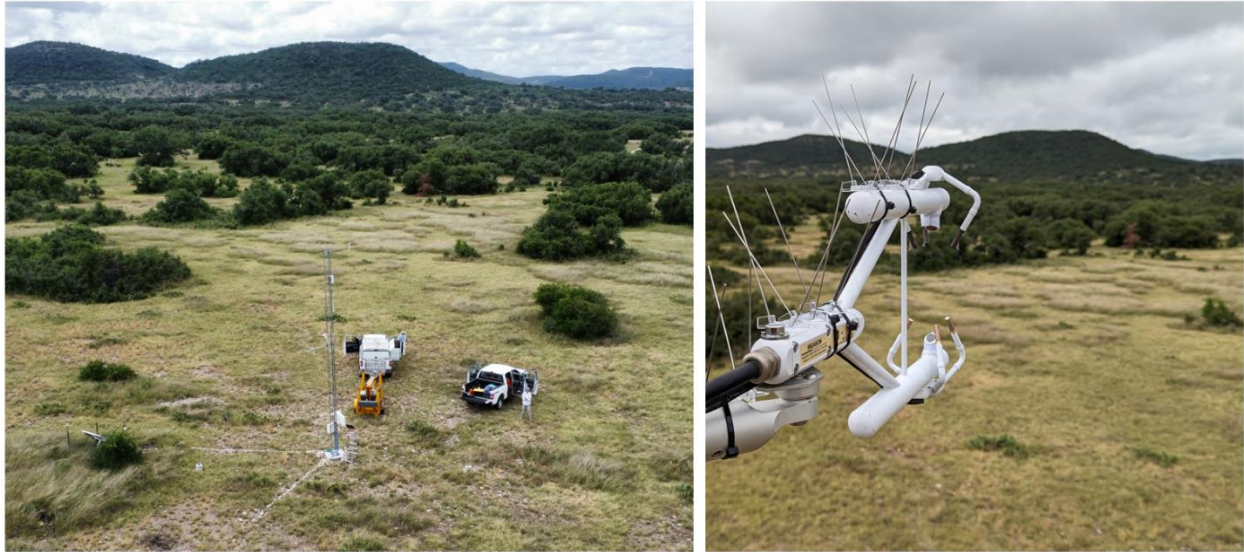


Figure 2.6. Field Photographs of Nueces (US-EA6) Site. (left) Eddy covariance station at the Nueces site; (right) photograph of Nueces site looking into direction of sonic azimuth showing general characteristics of oak-ashe juniper woody savanna ecosystem within measurement footprint.

Installation and maintenance of the Nueces site is summarized in Table 2.4 and detailed in the quarterly reports and included calibrating the IRGASON (Figure 2.7) and replacing a faulty 4-way radiometer. Moving forward, regular site visits will be performed at least twice a year to service the IRGASON (i.e., clean lenses, replace rain wicks, level and perform a zero-span), calibrate the rain gauge, clean radiometer lenses and re-level, and address any further issues. Additional site visits will be made on an as-needed basis.



Figure 2.7. Field Photographs of Nueces (US-EA6) Station Maintenance. (left) UT-BEG personnel performing a zero-span on the Nueces station IRGASON from a lift; (right) installation of ground-based sensors in soil pit #1 at the Nueces site (right).

Table 2.4 Nueces (US-EA6) Maintenance History

Date	Maintenance Performed
3/1/2023	Installed tower, datalogger, ground-based sensors, 4-way radiometer, PAR sensor, rain gauge, solar panel, and battery
4/12/2023	Re-installed solar panel wiring to troubleshoot power issue; replaced station battery; collected 3 soil samples near each of soil pits #1 and #2
7/6/2023	Installed EC100 and IRGASON (noted that CO ₂ concentration measurement seemed high at ~450 ppm); installed net radiometer (NR-Lite2) from US-EA5; swapped out desiccant in datalogger control box; replaced micro-SD memory card; tried unsuccessfully to fix malfunctioning 4-way radiometer (SN500SS)
7/19/2023	Installed new 4-way radiometer (SN500SS); calibrated rain gauge; performed a zero-span on IRGASON

3 Data Processing

3.1 Overview

The quality assurance and quality control (QA/QC) process for data from the Cibolo, Uvalde, and Nueces sites consists of three main steps (summarized in Figure 3.1). These steps are executed sequentially by 1) Campbell Scientific (on their datalogger; Section 3.2), 2) UT-BEG (in home offices; Sections 3.3 and 3.4) and 3) AmeriFlux (at their facility; Section 3.5).

Eddy Covariance Station

Raw Data: 10 Hz gas concentration and wind speed/direction and 0.2 Hz meteorological data collected at eddy covariance site
Half-Hourly Data: 30-min average of processed 10 Hz data and 0.2 Hz meteorological data

UT-BEG

BEG Filtered Data: 30-min data, filtered and de-spiked
Provisional ET Data: 30-min gap-filled data, energy fluxes and ET before and after Bowen-correction applied

AmeriFlux

BASE Product: 30-min data, QA/QC'd by AmeriFlux and published to their website
FLUXNET Product: 30-min gap-filled data with ecosystem parameters calculated (including ET and GPP)

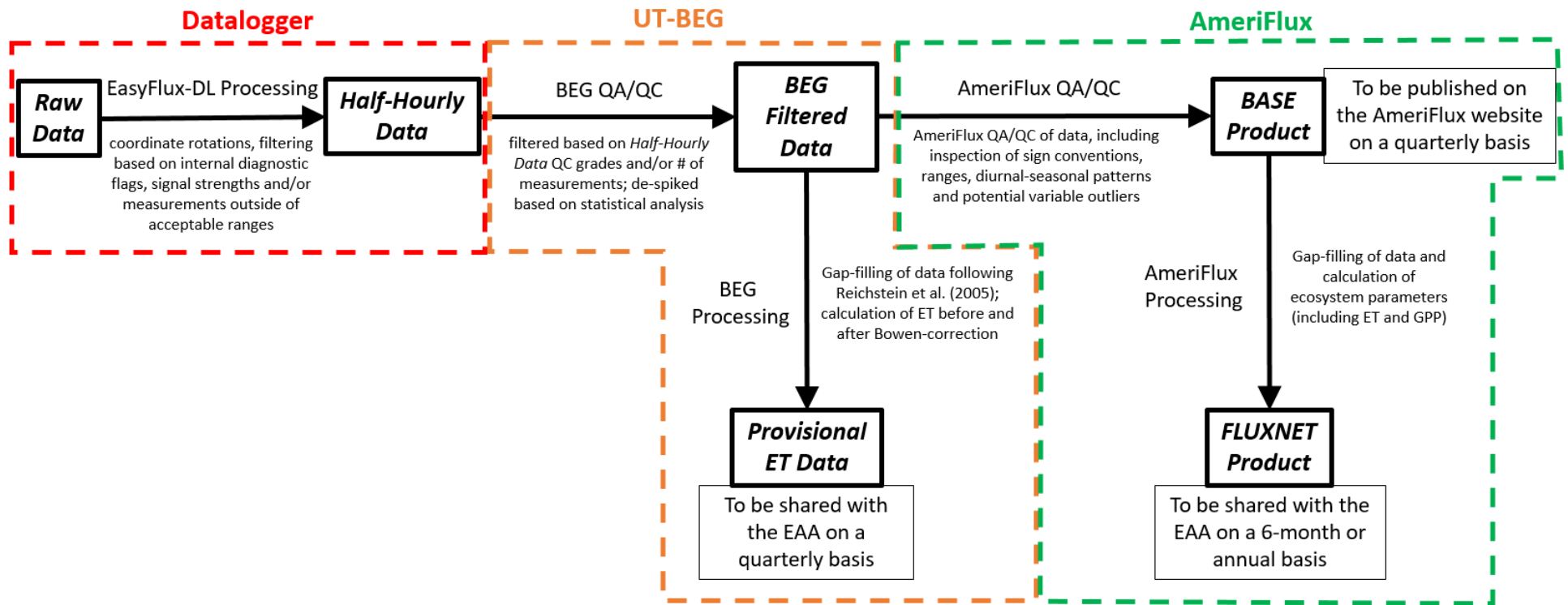


Figure 3.1. Eddy Covariance Data QA/QC and Processing Flowchart. Flowchart showing the different data QA/QC and processing steps and the different data products from the *Raw Data* collected on the data logger to the *Provisional ET Data* shared with the EAA and the *FLUXNET Product* produced by the AmeriFlux network.

3.2 EasyFlux-DL Processing (*Raw Data* → *Half-Hourly Data*)

The first QA/QC step is performed within the EasyFlux-DL program supplied by the eddy covariance vendor (Campbell Scientific, Inc., Logan, UT) and installed on the datalogger itself. Data collection and initial processing of raw data are described in Section 4.5 and the Appendices of the EasyFlux-DL CR3000OP and CR1KXOP manuals (Campbell Scientific, 2018 and 2022). Relevant information on EasyFlux-DL is summarized here. Gas concentrations, wind speed, and 3-D wind direction are measured at a frequency of 10-Hz (i.e., 10 measurements per second) (henceforth referred to as the *Raw Data*) and processed over 30-minute intervals (henceforth referred to as the *Half-Hourly Data*), with coordinate rotations applied every 5 minutes. Before calculating averages, the 10-Hz data are filtered based on diagnostic flags, signal strengths and/or measurements outside of acceptable ranges as defined by Campbell Scientific. Once the 30-minute averaged values are calculated, QC grades are assigned to fluxes of sensible heat (H), latent heat (LE), and carbon dioxide (CO₂; FC) based on a series of quality tests that explore (1) relative non-stationarity, or steady-state behavior over the 30-minute interval; (2) relative integral turbulence characteristics, or degree of development of turbulent conditions over the 30-minute interval; and, (3) the horizontal wind angle with respect to the sonic anemometer. The *Half-Hourly Data* is output in a series of tables depending on the EasyFlux-DL version (further details on the Campbell Scientific quality tests and output data tables can be found in Appendix F and Section 4.4 of the EasyFlux-DL manuals, respectively). For the CR3000 datalogger version of EasyFlux-DL (i.e., the Uvalde site and the Cibolo site pre-upgrade), *_Flux.dat and *_Flux_Notes.dat files are generated. For the CR1000X datalogger version of EasyFlux-DL (i.e., the Nueces site and the Cibolo site post-upgrade), *_Flux_AmeriFluxFormat.dat, *_Flux_CSFormat.dat, and *_Flux_Notes.dat files are generated. The differences between the output tables from different versions of EasyFlux-DL, combined with differences in sensor configuration between the different sites and before/after the upgrade at the Cibolo site, lead to slight differences in the ingestion and formatting of data at UT-BEG, discussed below.

3.3 BEG QA/QC (*Half-Hourly Data* → *BEG Filtered Data*)

3.3.1 Formatting and Converting Units

The BEG QA/QC is a multistep process that prepares the data for submission to AmeriFlux and for provisional processing for submission to EAA. All processing is done using Python scripts, which are available upon request. The first step for all three datasets is to import the *Half-Hourly Data* (*.dat files) as Pandas DataFrames and gap-fill missing time steps (e.g., those generated during periods when the station was without power) with rows of “NaN” (abbreviation for Not a Number) or -9999 (AmeriFlux preferred value in place of “NaN”). Next, for each site, the various *Half-Hourly Data* datasets and data from EAA weather stations are merged to obtain a complete set of variables (1) supported by AmeriFlux; (2) used to back-fill missing meteorological data (see Section 3.3.2); (3) used in the UT-BEG QA/QC process (e.g., the number of 10-Hz measurements for the flux parameters collected during a half-hour interval; see Section 3.3.3); and (4) requested by EAA (e.g., direct soil heat flux measurements at depth). For the Uvalde and pre-upgrade Cibolo datasets, this involves merging the *_Flux.dat, *_Flux_Notes.dat, and EAA weather data files. For the Nueces and post-upgrade Cibolo datasets, this involves merging the *_Flux_AmeriFluxFormat.dat and *_Flux_CSFormat.dat datasets. Once the respective datasets are merged, the variables of interest are sub-selected. For the Uvalde and pre-upgrade Cibolo datasets, columns are then added and filled in for “TIMESTAMP_START” and “TIMESTAMP_END” at each 30-minute interval by converting the “TIMESTAMP” for a given interval (from the *.dat file) from a format of YYYY-MM-DD HH:MM:SS to YYYYMMDDHHMM (AmeriFlux standard for timestamps) and variable abbreviations are changed to match AmeriFlux standard abbreviations (variable abbreviations are summarized in Table 3.1). For the pre-upgrade Cibolo dataset, blank columns are inserted for variables measured only after the site upgrade (e.g., maximum wind speed [WS_MAX], albedo [ALB], etc.) and populated with -9999 to facilitate combining the pre-upgrade and post-upgrade Cibolo datasets. Finally, unit conversions and sign convention changes are performed to match AmeriFlux standards. Specifically, soil water content (SWC) values are multiplied by a factor of 100 (for the Uvalde and pre-upgrade Cibolo datasets only) to convert units from volumetric ($\text{m}^3 \text{m}^{-3}$) to percent (%); vapor pressure deficit (VPD) values are multiplied by a factor of 10 to convert units kPa to hPa; the sign convention for momentum flux (TAU) is reversed (from positive to negative); and, QC grades are converted from Campbell

Scientific (CS) grades (1-9 with 1 being the highest quality) to the QC grades used by AmeriFlux that follow Foken et al. (2012) (0-2, with 0 being the highest quality). For the conversion of QC grades, CS grades of 1-3, 4-6, and 7-9 are set to 0, 1, and 2, respectively.

3.3.2 Backfilling SW_IN at Cibolo (US-EA4) and SW_IN and P at Uvalde (US-EA5)

Prior to the Cibolo site upgrade, incoming shortwave radiation (SW_IN) and photosynthetic photon density (PPFD_IN) were not measured, one of which is needed by AmeriFlux to perform ONEFlux processing (see Section 3.5.3). Those parameters were also not measured at the Uvalde site. In order to backfill SW_IN for these datasets, data collected from the nearby weather stations operated by EAA were used (BEX01WS for the Cibolo site and UVA02WS for the Uvalde site, <https://www.edwardsaquifer.org/science-maps/aquifer-data/weather-stations/>). For the Uvalde site, SW_IN is available from July 29, 2021, through the decommissioning of the station. For the Cibolo site, SW_IN is available from the installation of the station up until the upgrade, at which point a 4-way radiometer and PAR sensor were both installed. To correct for any bias between the SW_IN measurements between the BEX01WS weather station and the Cibolo site, a correlative analysis was performed for data collected from both sites *after* the Cibolo site was upgraded (i.e., between January 12, 2023, and December 31, 2023, when data from the 4-way radiometer at US-EA4 were available). The SW_IN measurements at the Cibolo site are consistently lower than at BEX01WS (Figure 3.2). The relationship between the two stations was used to correct SW_IN measurements from BEX01WS used to backfill the Cibolo dataset prior to the site upgrade. No such analysis was possible for the Uvalde site as that site only had a net radiometer installed.

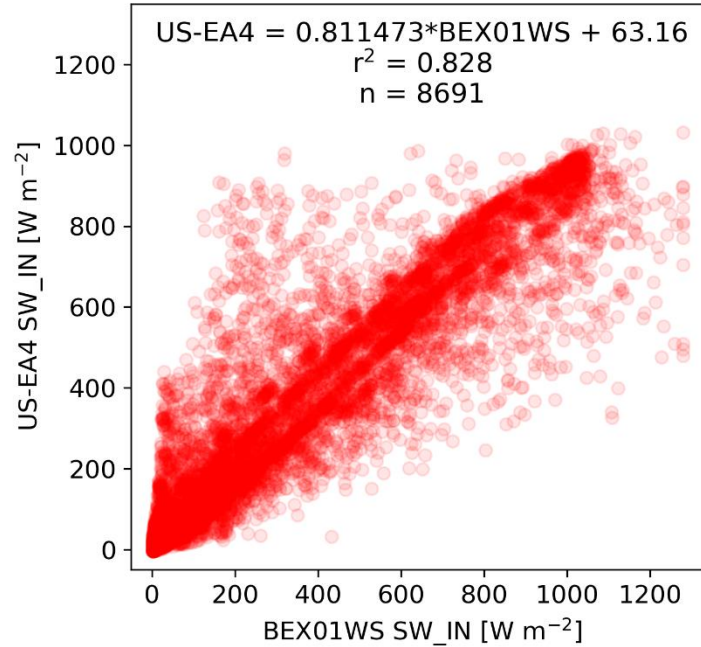


Figure 3.2. Comparison of SW_IN at Cibolo and BEX01WS. Correlation between SW_IN measured at EAA weather station (BEX01WS) and the Cibolo site (US-EA4) after the site upgrade from January 12, 2023, through December 31, 2023. This relationship was used to correct bias between the two sensors for SW_IN data collected at BEX01WS before the Cibolo upgrade.

Data collected from soil sensors at the Uvalde site do not exist from installation through September 21, 2021, at which point the sensors were checked and repaired. Due to the lack of SWC data during that period, ground heat flux (G) could not be calculated within the EasyFlux program on-site. An attempt was made to backfill G for the missing time period using SWC from UVA02WS along with soil temperature and soil heat flux data collected by the temperature averaging thermocouple (TCAV) and ground heat flux plates (HFP01), respectively, installed at the Uvalde site, using the following equations (outlined in Appendix H of the EasyFlux-DL CR3000OP operating manual):

$$G = G_{Depth} + \Delta_{storage} \quad \text{Eq. 3.1}$$

$$\Delta_{storage} = \frac{[c_s \rho_s (T_{soil,f} - T_{soil,i}) + c_w \rho_w (T_{soil,f} q_{v,f} - T_{soil,i} q_{v,i})] D}{\Delta t} \quad \text{Eq. 3.2}$$

where G_{Depth} is the calculated as the average soil heat flux at depth between the two ground heat flux plates installed at the site [W m^{-2}]; $\Delta_{storage}$ is the change in heat storage in the layer of soil above the soil heat flux measurement depth [W m^{-2}]; c_s is the specific heat of dry mineral soil at

the site [$870 \text{ J kg}^{-1} \text{ K}^{-1}$]; ρ_s is the soil bulk density at the site [$1,300 \text{ kg m}^{-3}$]; $T_{soil,f}$ is the average soil temperature at the end of the half-hour interval [$^{\circ}\text{C}$]; $T_{soil,i}$ is the average soil temperature at the beginning of the half-hour interval [$^{\circ}\text{C}$]; c_w is the specific heat of liquid water [$4,210 \text{ J kg}^{-1} \text{ K}^{-1}$]; ρ_w is the density of liquid water [$1,000 \text{ kg m}^{-3}$]; $q_{v,f}$ is the average volumetric soil water content at the end of the half-hour interval [$\text{m}^3 \text{ m}^{-3}$]; $q_{v,i}$ is the average volumetric soil water content at the beginning of the half-hour interval [$\text{m}^3 \text{ m}^{-3}$]; D is the depth below the surface at which the soil heat flux plates are buried [0.08 m]; and Δt is the time interval over which the change in heat storage is calculated [s]. However, the SWC data from UVA02WS were considerably different than the SWC data from the Uvalde site after the sensors were repaired (Figure 3.3). If SWC data can be obtained from a different weather station or remotely-sensed dataset (e.g., Soil Moisture Active Passive [SMAP]), then equations 3.1 and 3.2 could be used to calculate and backfill G as described above.

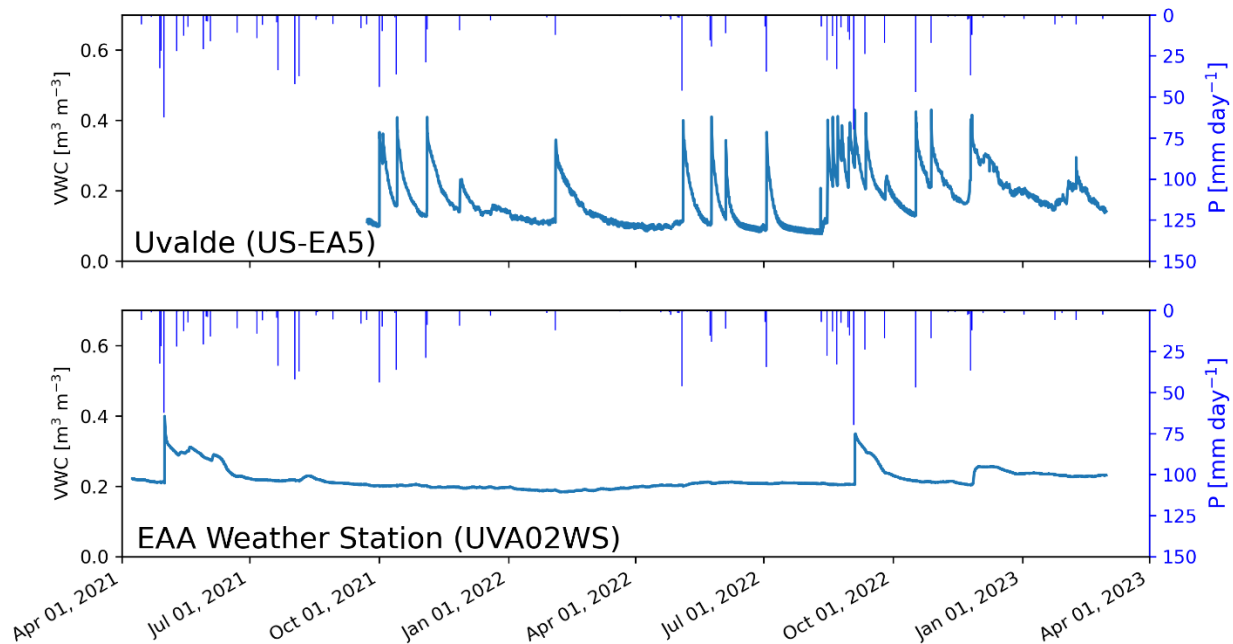


Figure 3.3. Comparison of SWC Measured at Uvalde Site and EAA Weather Station. Time series comparison of SWC measured at the Uvalde site (US-EA5) and the EAA Weather Station (UVA02WS) for the duration of the Uvalde site dataset.

The rain gauge at the Uvalde site began to malfunction sometime around January 1, 2022. Precipitation data in the Uvalde dataset from January 1, 2022, through the decommissioning of the station (March 1, 2023) was also backfilled by data collected at the nearby EAA weather station (UVA02WS).

3.3.3 Filtering

After the Pandas DataFrames are formatted, several steps of progressive filtering are performed to remove questionable data. The first stage involves removing data based on AmeriFlux standard expected limits (summarized in Table 3.1), that follow either physical laws (e.g., wind direction is limited between 0 and 360°), or values that would indicate sensor failure (e.g., fluxes of LE and H outside the range of -450 to 900 W m⁻², which would not be physically possible given our knowledge of incoming radiation).

The next step of filtering involves detecting and removing spikes for carbon flux (FC), latent heat flux (LE), sensible heat flux (H), and ground heat flux (G). Spike detection and removal is performed by removing any data point outside of two standard deviations from the mean, calculated ± 7 days from the data point in question. For data following a Gaussian (normal) distribution, which we are assuming, this filtering would capture 95% of data, thereby removing only a small percentage. Mean values are calculated separately for daytime and nighttime periods (with daytime defined as net radiation [NETRAD] > 20 W m⁻²).

Next, half-hourly values calculated from high frequency data (i.e., FC, LE and H) are filtered based on QC grades and the number of 10-Hz measurements collected within each half-hour period. Specifically, any half-hour measurement with a relatively poor QC grade of 2 in the AmeriFlux format (7-9 in CS format) and/or with less than 90% collection over a 30-min interval (i.e., < 16,200 measurements of the possible 18,000 in a half-hour interval) are replaced by “NaN” or -9999. The remaining data are considered formatted and filtered; this *BEG Filtered Data* product is complete and ready for (1) provisional gap-filling and calculation of ET and Bowen-corrected fluxes (see Section 3.4) and (2) submission to AmeriFlux for their QA/QC and processing (see Section 3.5).

Table 3.1. Physical and Expected Limits for AmeriFlux Variables

Variable	Parameter	units	Physical		Expected ¹	
			min	max	min	max
CO2	CO ₂ mole fraction	μmolCO ₂ mol ⁻¹			150	1,200
H2O	average H ₂ O molar mixing ratio (dry basis)	μmolH ₂ O mol ⁻¹			0	100
FC	CO ₂ flux after corrections	μmolCO ₂ m ⁻² s ⁻¹			-100	100
LE	latent heat flux after corrections	W m ⁻²			-450	900
H	sensible heat flux after corrections	W m ⁻²			-450	900
G	calculated heat flux at the ground surface	W m ⁻²			-250	400
SG	change in heat storage in the soil above the soil heat flux plates during the averaging interval	W m ⁻²			-100	250
WD	average wind direction	degrees	0	360		
WS	average wind speed	m s ⁻¹			0	40
WS_MAX ^{II}	maximum wind speed	m s ⁻¹			0	50
USTAR	frictional velocity	m s ⁻¹			0	8
ZL	stability	nondimensional			N/A	N/A
TAU	momentum flux	kg m ⁻¹ s ⁻²			-10	-2
MO_LENGTH	Monin-Obukhov length	m			N/A	N/A
PA	average atmospheric pressure	kPa			60	105
TA_1_1_1	average air temperature from EC100 temperature probe	°C			-50	50
RH_1_1_1	average relative humidity calculated from EC100 temperature probe, H ₂ O, and pressure	%	0	100		
TA_1_1_2	average air temperature calculated from sonic temperature, H ₂ O, and pressure	°C			-50	50
RH_1_1_2 ^{II}	average relative humidity calculated from sonic temperature, H ₂ O, and pressure	%	0	100		
VPD	vapor pressure deficit	hPa	0	80		
T_SONIC	average sonic temperature	°C			-50	50
TS_1_1_1	average soil temperature for sensor #1	°C			-40	65
TS_1_1_2	average soil temperature for sensor #2	°C			-40	65
TS_2_1_1 ^{II}	average soil temperature for sensor #3	°C			-40	65
SWC_1_1_1	average soil water content for sensor #1	%	0	100		
SWC_1_1_2	average soil water content for sensor #2	%	0	100		
SWC_2_1_1 ^{II}	average soil water content for sensor #3	%	0	100		
ALB ^{II}	albedo	%	0	100		
NETRAD ^{IV}	net radiation from NRLite2 net radiometer	W m ⁻²			-200	1,100
NETRAD_1_1_1 ^{II}	net radiation from NRLite2 net radiometer	W m ⁻²			-200	1,100
NETRAD_1_1_2 ^{II}	net radiation from SN500SS 4-way radiometer	W m ⁻²			-200	1,100
PPFD_IN ^{II}	photosynthetic photon density	μmolPhoton m ⁻² s ⁻¹			0	2,400
SW_IN_1_1_1 ^{III}	incoming short-wave radiation	W m ⁻²			0	1,300
SW_IN_F_1_1_1 ^{III}	incoming short-wave radiation (gap-filled)	W m ⁻²			0	1,300
SW_IN_2_1_1 ^{IV}	incoming short-wave radiation (from separate location/station)	W m ⁻²			0	1,300
SW_IN ^V	incoming short-wave radiation	W m ⁻²			0	1,300
SW_OUT ^{II}	outgoing short-wave radiation	W m ⁻²			0	800
LW_IN ^{II}	incoming long-wave radiation	W m ⁻²			50	600
LW_OUT ^{II}	outgoing long-wave radiation	W m ⁻²			100	750
P ^{II}	precipitation in output interval	mm			0	50

P_1_1_1 ^{Iv}	precipitation in output interval	mm		0	50
P_2_1_1 ^{Iv}	precipitation in output interval	mm		0	50
P_1 ^{Iv}	precipitation in output interval (aggregated)	mm		0	50

^IAmeriFlux standard limits

^{II}Cibolo (US-EA4) and Nueces (US-EA6) only

^{III}Cibolo (US-EA4) only

^{IV}Uvalde (US-EA5) only

^VNueces (US-EA6) only

3.4 BEG Processing (*BEG Filtered Data* → *Provisional ET Data*)

3.4.1 Gap-Filling

Gap-filling is the first step performed on the *BEG Filtered Data* to prepare the *Provisional ET Data* product. Linear interpolation is used to gap-fill FC, LE, H, and G for periods less than or equal to 2 hours. Longer gaps for FC, LE, H, and G are filled following the methods outlined in Appendix A of Reichstein et al. (2005). Specifically, for a missing flux value, if NETRAD, VPD and ambient temperature (TA) are available during the half-hour interval in question, then the missing flux value is replaced by the average value under similar meteorological conditions (defined as NETRAD, VPD, and TA values within 50 W m^{-2} , 5.0 hPa, and $2.5 \text{ }^{\circ}\text{C}$, respectively) within a ± 7 -day time window ± 30 min from the time of day for the data point being analyzed. If VPD or TA are not available, the value is replaced by the average value under similar net radiation conditions only (NETRAD within 50 W m^{-2}).

3.4.2 ET Calculation and Bowen-Correction of LE and H

Once data are filtered and gap-filled, evapotranspiration (*ET*) is calculated according to the following equation:

$$ET = \frac{LE}{\lambda \rho_w} \quad \text{Eq. 3.3}$$

where *LE* is the latent heat flux [W m^{-2}], λ is the latent heat of vaporization of water [$2,501 \text{ KJ kg}^{-1}$] and ρ_w is the density of water [$1,000 \text{ kg m}^{-3}$]. The latent heat (*LE*) flux is calculated within the EasyFlux program on the datalogger for each half-hourly interval according to the following equation:

$$LE = \lambda \overline{w'q'} \quad \text{Eq. 3.4}$$

where $\overline{w'q'}$ is the covariance between vertical speed (*w*) and water density (*q*). Due to factors still being studied in the scientific community, the surface energy fluxes are often underestimated by 10-30% relative to the available energy (Foken et al., 2012; Wilson et al., 2002). The parameters *LE* and *H* can be adjusted to force closure while maintaining a constant Bowen ratio (β), which is

the ratio between H and LE (Blanken et al., 1997; Lee, 1998; Twine et al, 2000), according to the following equations:

$$\beta = \frac{H}{LE} \quad \text{Eq. 3.5}$$

$$LE_{corr} = \frac{(R_n - G)}{1 + \beta} \quad \text{Eq. 3.6}$$

$$H_{corr} = LE_{corr} \times \beta \quad \text{Eq. 3.7}$$

where R_n is the net radiation [W m^{-2}], averaged between the 4-way radiometer and the net radiometer (if both are available) and LE_{corr} and H_{corr} are Bowen-corrected latent heat flux and sensible heat flux, respectively [W m^{-2}]. Bowen-corrections of H and LE are only performed under daytime conditions (average $R_n > 20 \text{ W m}^{-2}$) and when β is above 0.6, both conditions which were somewhat arbitrarily chosen. Once Bowen-corrected LE and H are calculated, a Bowen-corrected evapotranspiration (ET_{corr}) can be calculated according to the following equation:

$$ET_{corr} = \frac{LE_{corr}}{\lambda \rho_w} \quad \text{Eq. 3.8}$$

If the conditions described above for performing a Bowen-correction are not met, ET_{corr} is equal to ET calculated in Equation 3.3.

3.4.3 Provisional ET Data Product

After ET has been calculated and Bowen-corrections have been applied, a subset of the dataset is generated and provided to the EAA, referred to as the *Provisional ET Data* product. This dataset focuses on ET , the energy balance components, and common meteorological parameters measured at the stations. For certain meteorological parameters (e.g., ambient air temperature and soil heat flux within an individual pit), values included in the *Provisional ET Data* product are averages of measurements from replicate sensors (Table 3.2). Moving forward, the *Provisional ET Data* product will be transmitted to the EAA on a quarterly basis and will be noted as **provisional**.

The *Provisional ET Data* datasets for the Cibolo (US-EA4), Uvalde (US-EA5), and Nueces (US-EA6) sites that are included with this report have been published to the Texas Data Repository Dataverse (McKinney, 2024; <https://doi.org/10.18738/T8/1NSBMG>).

Table 3.2 Provisional ET Data Variable Metadata

Symbol	Variable	Unit	Instrument	Collection Rate
P	precipitation	mm	TE525	10 Hz; totaled over 30 min intervals
ET	evapotranspiration	mm hr ⁻¹	IRGASON ^I	10 Hz; averaged over 30 min intervals
ETcorr	Bowen-corrected evapotranspiration	mm hr ⁻¹	IRGASON ^I	10 Hz; averaged over 30 min intervals
LE	latent heat flux	W m ⁻²	IRGASON ^{II}	10 Hz; averaged over 30 min intervals
LEcorr	Bowen-corrected latent heat flux	W m ⁻²	IRGASON ^{II}	10 Hz; averaged over 30 min intervals
H	sensible heat flux	W m ⁻²	IRGASON ^{II}	10 Hz; averaged over 30 min intervals
Hcorr	Bowen-corrected sensible heat flux	W m ⁻²	IRGASON ^{II}	10 Hz; averaged over 30 min intervals
NETRAD	net radiation	W m ⁻²	NRLite2/SN500SS ^{III}	5 sec; averaged over 30 min intervals
G	ground heat flux	W m ⁻²	ground-based sensors ^{IV}	5 sec; averaged over 30 min intervals
AIRTEMP	ambient air temperature	°C	EC100 temperature probe & IRGASON ^V	10 Hz; averaged over 30 min intervals
AIRPRES	atmospheric pressure	kPa	EC100 barometer	10 Hz; averaged over 30 min intervals
RH	relative humidity	%	EC100 temperature probe & IRGASON ^V	10 Hz; averaged over 30 min intervals
WNDDIR	wind direction	°	IRGASON	10 Hz; averaged over 30 min intervals
WNDSPD	wind speed	m s ⁻¹	IRGASON	10 Hz; averaged over 30 min intervals
SLVWC_PIT1	soil water content in pit #1	m ³ m ⁻³	CS655 ^{VI}	5 sec; averaged over 30 min intervals
SLVWC_PIT2	soil water content in pit #2	m ³ m ⁻³	CS655 ^{VI}	5 sec; averaged over 30 min intervals
SLTMP_PIT1	soil temperature in pit #1	°C	CS655 ^{VI}	5 sec; averaged over 30 min intervals
SLTMP_PIT2	soil temperature in pit #2	°C	CS655 ^{VI}	5 sec; averaged over 30 min intervals
SLHTFLX_PIT1	soil heat flux at depth in pit #1	W m ⁻²	HFP01/HFP01SC ^{VI}	5 sec; averaged over 30 min intervals
SLHTFLX_PIT2	soil heat flux at depth in pit #2	W m ⁻²	HFP01/HFP01SC ^{VI}	5 sec; averaged over 30 min intervals
SW_IN	incoming shortwave radiation	W m ⁻²	SN500SS ^{VII}	5 sec; averaged over 30 min intervals
PAR_IN	incoming photosynthetically-active radiation	μmol m ⁻² s ⁻¹	CS310	5 sec; averaged over 30 min intervals

^ICalculated using *LE* and *LEcorr* values (see Section 3.4.2)

^{II}Calculated based on covariance between H₂O concentrations and vertical wind speed

^{III}Averaged value of NRLite2 and SN500SS sensors for Cibolo (US-EA4) and Nueces (US-EA6) sites; NRLite2 value for Uvalde (US-EA5) site

^{IV}Calculated using ground heat flux measurements taken at depth and soil water content and soil temperature above soil heat flux plates

^VAveraged value between measurements from EC100 temperature probe and calculated values from sonic temperature, H₂O and pressure

^{VI}When applicable, averaged value between multiple sensors at the same depth within the same pit

^{VII}Back-filled from EAA weather station data for Uvalde site and pre-upgrade Cibolo site (see Section 3.3.2)

3.5 AmeriFlux QA/QC & Processing

3.5.1 Overview

In addition to being provisionally processed for EAA, the *BEG Filtered Data* product is sent to AmeriFlux for further QA/QC processing (to produce the *BASE Product*) and standardized gap filling and calculation of ecosystem parameters (to produce the *FLUXNET Product*). Details about the AmeriFlux data processes and pipelines are summarized below and additional information can be found on the AmeriFlux website (<https://ameriflux.lbl.gov/data/flux-data-products/>).

3.5.2 AmeriFlux QA/QC (*BEG Filtered Data* → *BASE Product*)

AmeriFlux QA/QC assesses both the format and quality of the submitted *BEG Filtered Data*. The formatting QA/QC involves a series of format tests, such as the assessment of timestamps, variable names and missing values. It is a fully automated process, with results of the format tests returned to UT-BEG the same day that *BEG Filtered Data* are submitted. The quality QA/QC performed by AmeriFlux identifies potential issues with data quality and is considered to be complementary to the primary QA/QC performed by the site team (e.g., UT-BEG). Data are assessed using a series of test modules that investigate sign conventions, timestamp alignments, trends, step changes, outliers based on historical ranges, multivariate comparisons (e.g., TA versus sonic temperature [T_SONIC] and SW_IN versus PPFD_IN), diurnal/seasonal patterns, friction velocity [USTAR] filtering, and variable availability (Chu et al., 2023; Pastorello et al., 2014 & 2020). The AmeriFlux data team iterates with UT-BEG until the submitted data pass all format and quality QA/QC tests, at which point the dataset is published on the AmeriFlux website as the *BASE Product* (QA/QC'd, but not gap-filled and without calculations of ET) and returned to UT-BEG. The quality QA/QC step can take anywhere from weeks to months depending on the availability of AmeriFlux personnel.

3.5.3 AmeriFlux ONEFlux Processing (*BASE Product* → *FLUXNET Product*)

After the dataset passes AmeriFlux QA/QC, the resulting *BASE Product* is processed using the ONEFlux data processing code package developed by FLUXNET (a global network of regional

eddy covariance networks, including AmeriFlux) to gap-fill and calculate ecosystem parameters (including ET), resulting in the final, *FLUXNET Product*. The ONEFlux data processing pipeline consists of five major steps: (1) thorough data QC checks; (2) filtering of low-turbulence periods based on calculations of friction velocity (i.e., USTAR) thresholds; (3) gap-filling of meteorological and flux measurements; (4) partitioning of CO₂ fluxes (FC) into respiration and photosynthesis; and (5) calculating a correction factor for energy fluxes at the site (<https://fluxnet.org/data/fluxnet2015-dataset/data-processing/>; Pastorello et al., 2020). ONEFlux QA/QC procedures include checks of single variable trends at multiple temporal resolutions, multiple variable relationships (i.e., variables that should vary comparably), and more specialized tests, such as comparing measured radiation to the maximum expected radiation for a given location. Sensible (H) and latent heat (LE) fluxes are gap-filled using the marginal distribution sampling (MDS) method (Reichstein et al., 2005) and corrected using a Bowen ratio method. Random uncertainties in H and LE are also estimated at a half-hourly resolution using two hierarchical methods, one based on a direct standard deviation, and the other on a median standard deviation. Net ecosystem exchange (NEE) is filtered with an ensemble of USTAR thresholds and subsequently gap-filled using the MDS technique (Reichstein et al., 2005). Half-hourly NEE is then partitioned into its two components: gross primary production (GPP), or photosynthesis, and ecosystem respiration (RECO) using two different methods. The first method is a nighttime-based approach (Reichstein et al., 2005), while the second method is based on daytime data (Lasslop et al., 2010). This final, standardized, processed *FLUXNET Product* will be posted to the AmeriFlux website and returned to UT-BEG, who will then transmit the data to EAA as the **final** dataset. Moving forward, transmission of the *FLUXNET Product* is expected to occur on a 6-month or annual basis.

4 Results and Discussion

4.1 Data Processing

The QA/QC and processing steps described here and applied to the eddy covariance datasets led to progressive removal of flux data through the filtering and de-spiking processes, followed by gap filling processes of flux values.

4.1.1 Cibolo Site (US-EA4)

The Cibolo site was without power from January 19 through March 9, 2022. This six-week gap is too long to fill in using conventional gap-filling techniques, so a baseline amount of missing flux data existed for the Cibolo site (~4.7% of the total data through December 31, 2023; represented as a dashed horizontal line in Figure 4.1). Additional gaps in data collection occurred due to precipitation events and or obstructions to the infrared gas analyzer (such as bird droppings). The filtering and de-spiking steps applied to the Cibolo dataset resulted in removal of an additional ~40% of LE measurements, with the largest source of removal of flux measurements stemming from bad QC grades (“QC Flag Filter”). The majority of these missing and removed data points are filled in by the short and long gap-filling steps, resulting in only 13% of LE measurements missing by the end of data processing (Figure 4.1 and Table 4.1).

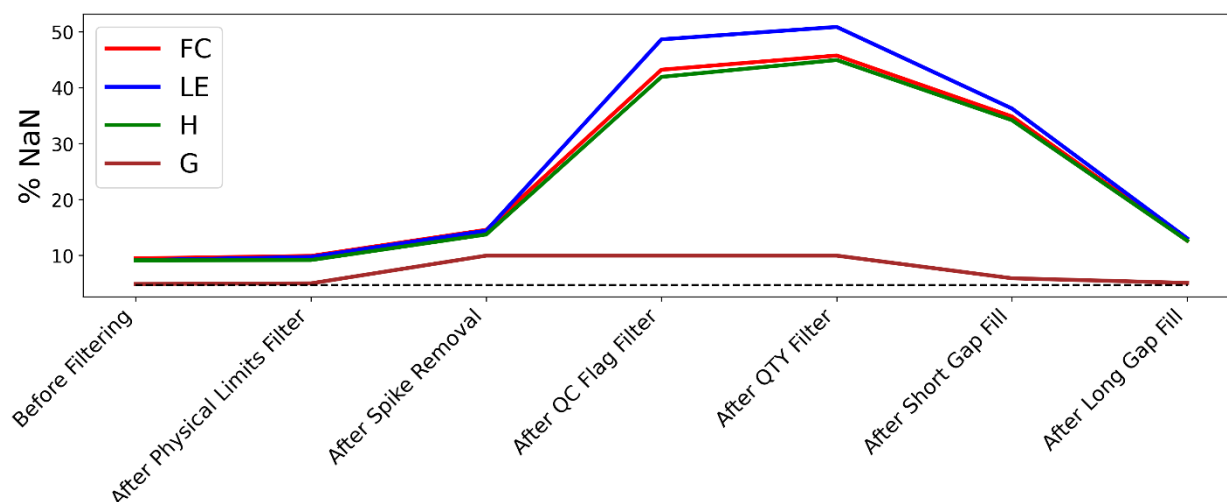


Figure 4.1. Percentage of Missing Data for Cibolo Throughout QA/QC and Processing. Percentage of half-hourly NaN values for flux and energy balance parameters at the Cibolo site (US-EA4) at the different QA/QC and processing steps; the horizontal dashed line represents the baseline percentage of NaN values from the gap in data collection from January 19 through March 9, 2022.

Table 4.1. Amount of Missing Flux Measurements for Cibolo During QA/QC Steps

Step	FC #	FC %	LE #	LE %	H #	H %	G #	G %
Unprocessed	4,717	9.5	4,553	9.1	4,553	9.1	2,434	4.9
Physical Filter	4,938	9.9	4,848	9.7	4,571	9.2	2,490	5.0
Spike Removal	7,268	14.6	7,189	14.4	6,854	13.7	4,964	9.9
QC Filter	21,565	43.2	24,276	48.7	20,925	41.9	4,964	9.9
QTY Filter	22,833	45.8	25,386	50.9	22,433	45.0	4,964	9.9
Short Gap-fill	17,388	34.8	18,103	36.3	17,061	34.2	2,944	5.9
Long Gap-fill	6,293	12.6	6,511	13.0	6,304	12.6	2,530	5.1

4.1.2 Uvalde Site (US-EA5)

No major gaps in data collection occurred at the Uvalde site throughout its operation, although ground heat flux (G) was not calculated until the soil sensors were repaired in September 2021, leading to a baseline amount of missing G values (~24%). Before any processing, less than 2% of the remaining flux and energy balance measurements were missing, likely due to precipitation and/or obstructions to the infrared gas analyzer. The filtering and de-spiking steps applied to the Uvalde dataset resulted in removal of an additional ~33% of LE measurements, 27% of which were re-filled by the gap-filling procedures (Figure 4.2 and Table 4.2).

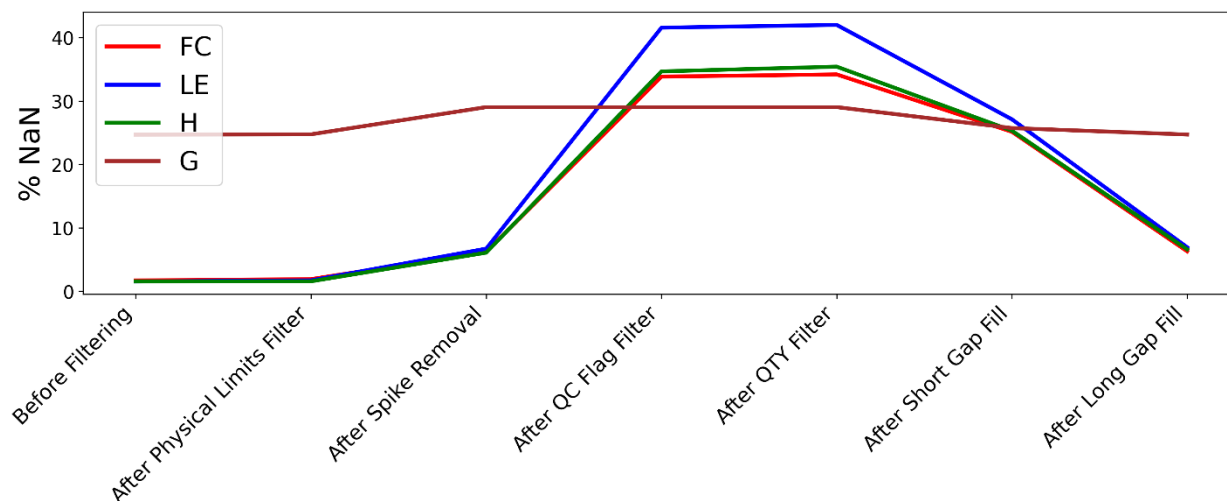


Figure 4.2. Percentage of Missing Data for Uvalde Throughout QA/QC and Processing. Percentage of half-hourly NaN values for flux and energy balance parameters at the Uvalde site (US-EA5) at the different QA/QC and processing steps.

Table 4.2. Amount of Missing Flux Measurements for Uvalde During QA/QC Steps

Step	FC #	FC %	LE #	LE %	H #	H %	G #	G %
Unprocessed	552	1.7	501	1.5	501	1.5	8,029	24.7
Physical Filter	617	1.9	555	1.7	506	1.6	8,045	24.7
Spike Removal	2,017	6.2	2,181	6.2	1,977	6.1	9,441	29.0
QC Filter	11,006	33.8	13,515	33.8	11,272	34.7	9,441	29.0
QTY Filter	11,118	34.2	13,658	34.2	11,516	35.4	9,441	29.0
Short Gap-fill	8,175	25.1	8,816	25.1	8,233	25.3	8,366	25.7
Long Gap-fill	2,047	6.3	2,252	6.3	2,146	6.6	8,035	24.7

4.1.3 Nueces Site (US-EA6)

Due to obstructions of the infrared gas analyzer and issues with deployment of the IRGASON and associated hardware (EC100) at the Nueces site, ~5% of the flux measurements were missing prior to the application of any filtering. The filtering and de-spiking steps resulted in removal of an additional ~40% of LE measurements, ~37% of which were gap-filled (Figure 4.3 and Table 4.3).

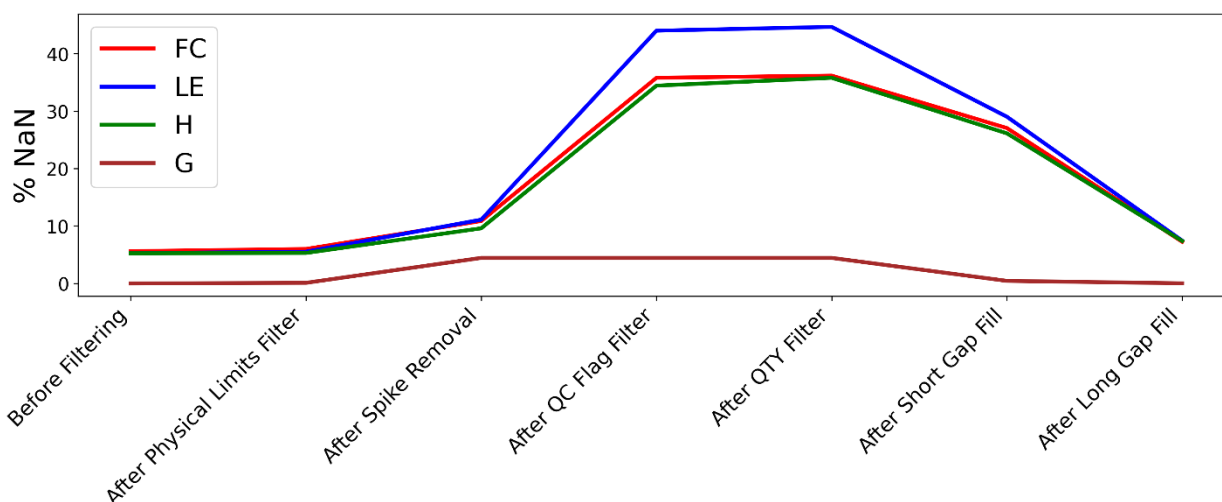


Figure 4.3. Percentage of Missing Data for Nueces Throughout QA/QC and Processing. Percentage of half-hourly NaN values for flux and energy balance parameters at the Nueces site (US-EA6) at the different QA/QC and processing steps.

Table 4.3. Amount of Missing Flux Measurements for Nueces During QA/QC Steps

Step	FC #	FC %	LE #	LE %	H #	H %	G #	G %
Unprocessed	444	5.6	417	5.3	417	5.3	0	0.0
Physical Filter	475	6.0	437	5.5	420	5.3	8	0.1
Spike Removal	861	10.9	879	11.1	760	9.6	352	4.4
QC Filter	2,835	35.8	3,485	44.0	2,727	34.4	352	4.4
QTY Filter	2,865	36.2	3,537	44.7	2,835	35.8	352	4.4
Short Gap-fill	2,142	27.0	2,298	29.0	2,069	26.1	35	0.44
Long Gap-fill	575	7.3	590	7.4	586	7.4	2	0.02

4.1.4 Summary of Results of Processing Steps

The effects of the filtering and gap-filling techniques used on the datasets can be seen by visually inspecting timeseries of the LE datasets (Figures 4.4 through 4.9). Before any processing, spikes in LE reached or exceeded $\pm 10,000 \text{ W m}^{-2}$, well beyond the expected limits for latent heat

flux. After applying the initial filter to remove data outside of expected limits (< -450 and > 900 W m^{-2} for LE), the general trend of LE can be deciphered, although ample spikes remained. De-spiking the data removed measurements outside of the expected trend of LE based on the season and precipitation events. Filtering the LE data based on QC grades and the number of 10 Hz measurements in each half-hour interval (“QTY Filter”) led to progressive removal of LE measurements, but did not affect the overall trend in LE. Gap-filling of the data led to a much more complete dataset, and did not result in any LE measurements outside of the general trend established by the de-spiking and filtering techniques.

The efficacy of the gap-filling techniques used here is demonstrated through the filling of missing LE data during a multi-day freeze at the Cibolo site (US-EA4) at the end of January 2023 (Figure 4.5) and a multi-day gap in collection at the Nueces site (US-EA6) in September 2023 (Figures 4.8 and 4.9), most likely the result of bird droppings on the infrared gas analyzer.

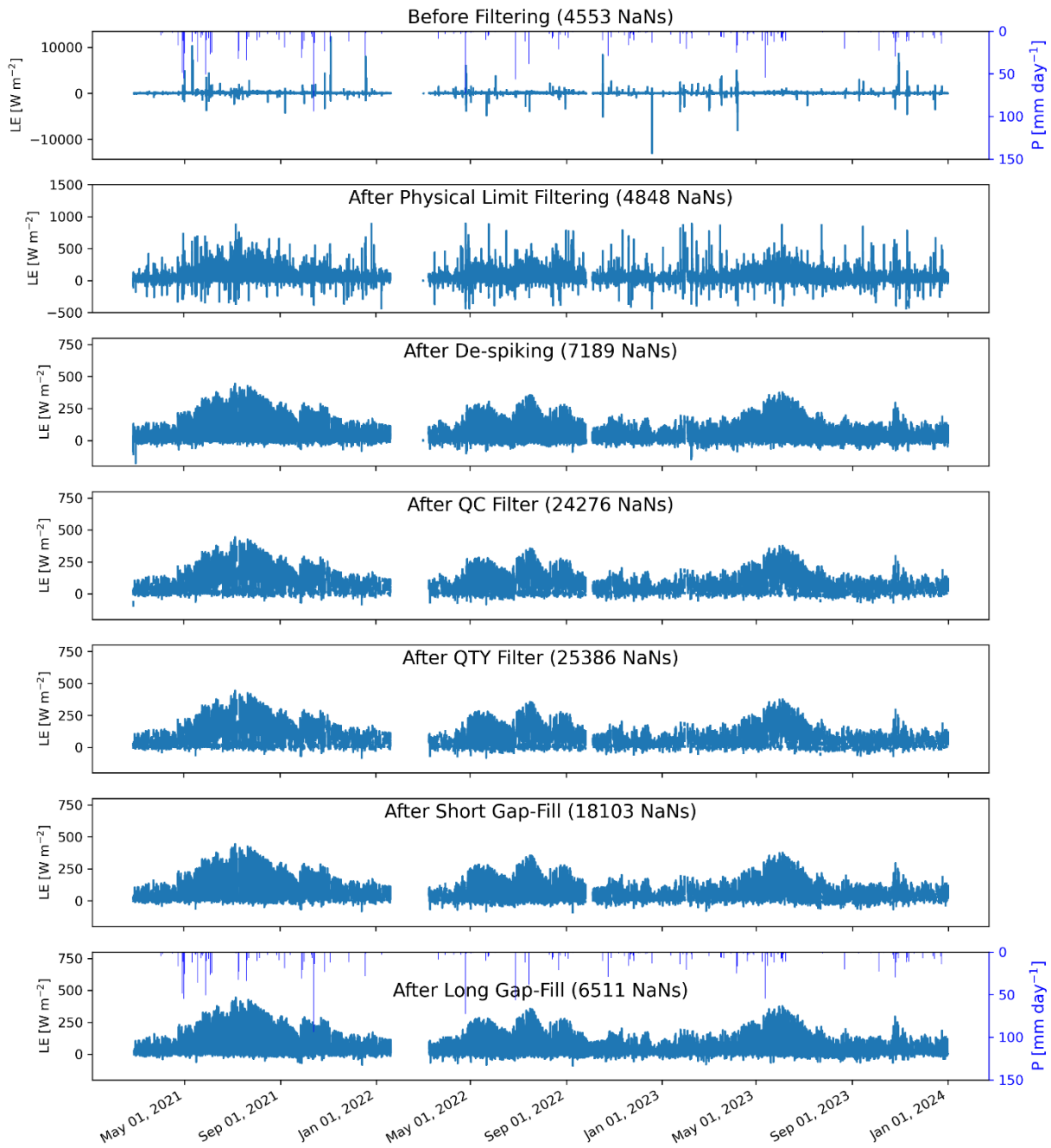


Figure 4.4. Timeseries of LE Data for Cibolo at Each QA/QC and Processing Step. Half-hourly LE measurements at the Cibolo site (US-EA4) before any processing (top) and after each successive processing step; daily precipitation is included on the secondary y-axis for the unprocessed (top) and final (bottom) datasets and the number of half-hourly NaNs is included for each step.

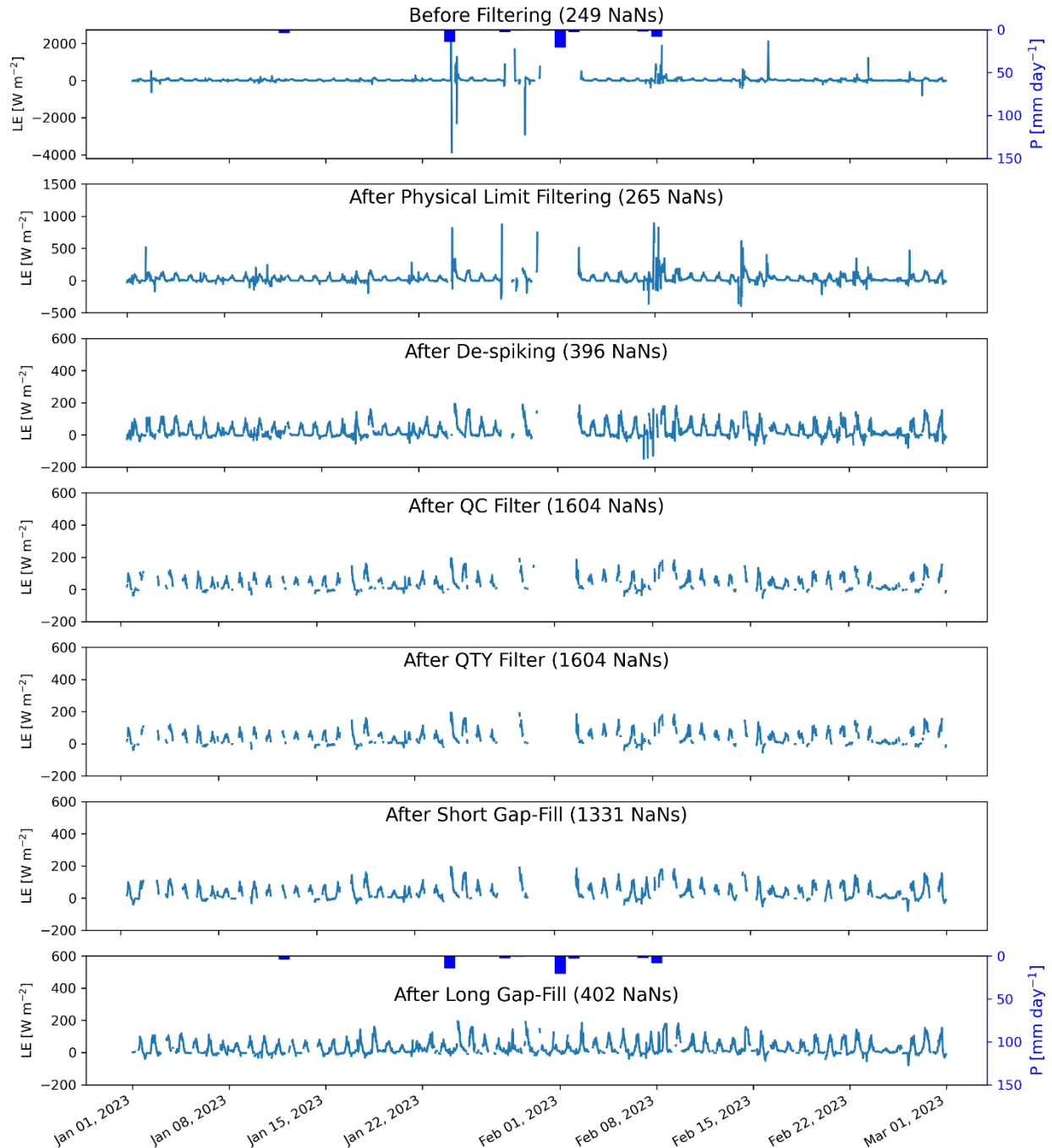


Figure 4.5. Subset of LE Data for Cibolo at Each QA/QC and Processing Step. Subset of half-hourly LE measurements at the Cibolo site (US-EA4) from January 1 through March 1, 2023, for the unprocessed data (top) and after each processing step, highlighting the gap in data collection at the end of January 2023 due to a multi-day freeze; daily precipitation is included on the secondary y-axis for the unprocessed (top) and final (bottom) datasets and the number of half-hourly NaNs for this two-month period is included for each step.

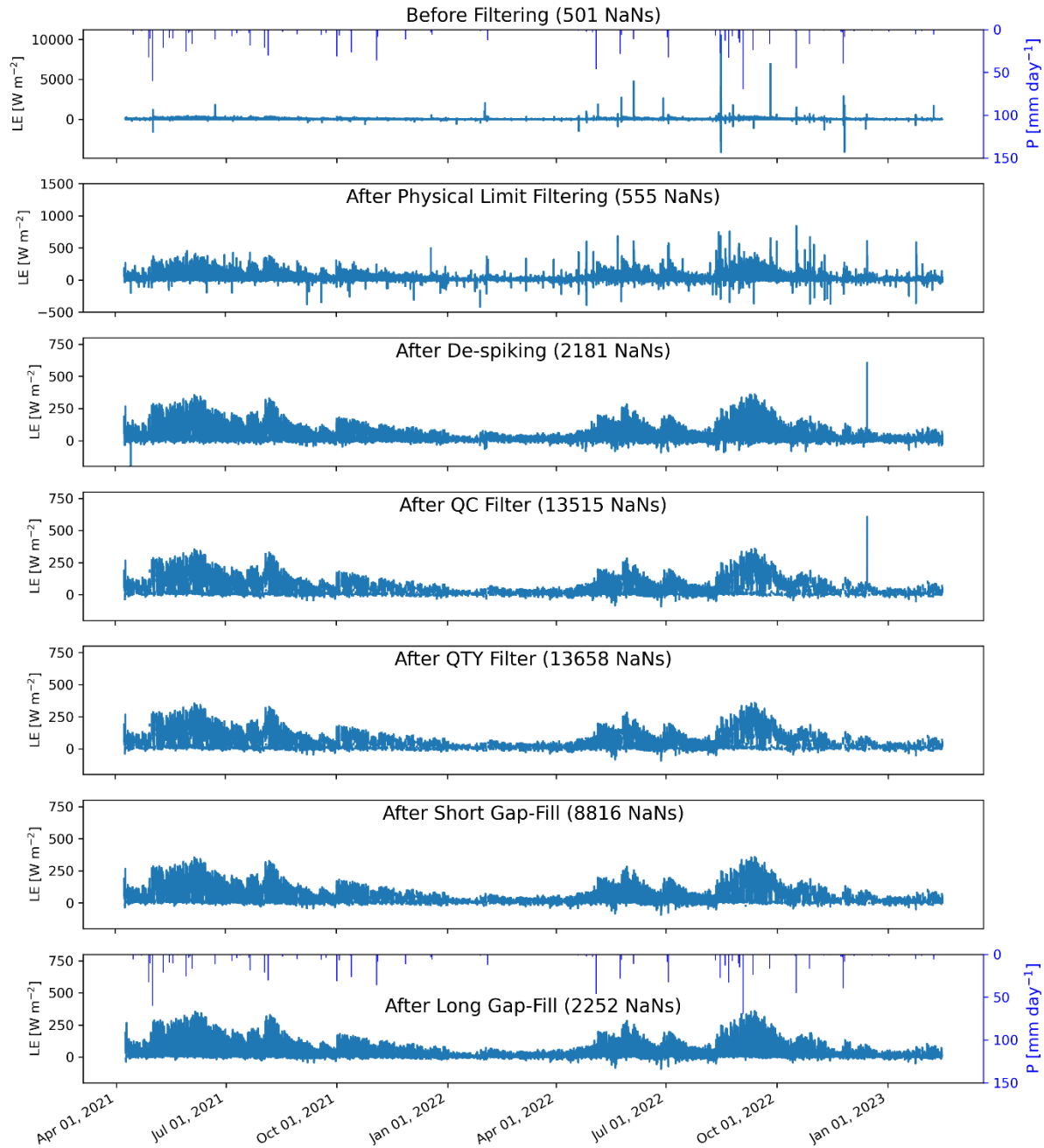


Figure 4.6. Timeseries of LE Data for Uvalde at Each QA/QC and Processing Step. Half-hourly LE measurements at the Uvalde site (US-EA5) before any processing (top) and after each successive processing step; daily precipitation is included on the secondary y-axis for the unprocessed (top) and final (bottom) datasets and the number of half-hourly NaNs is included for each step.

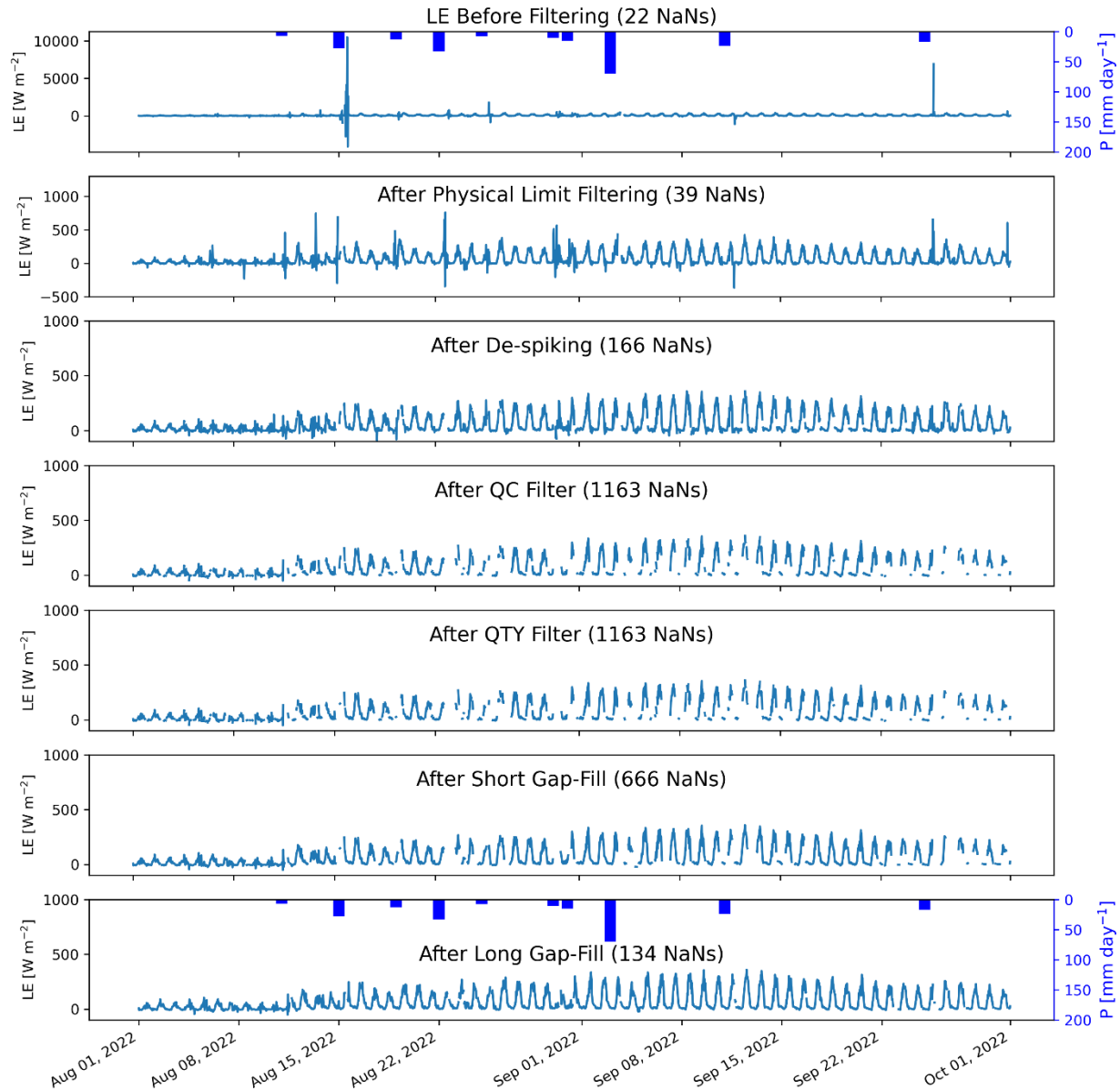


Figure 4.7. Subset of LE Data for Uvalde at Each QA/QC and Processing Step. Subset of half-hourly LE measurements at the Uvalde site (US-EA5) from August 1 through October 1, 2022, for the unprocessed data (top) and after each processing step; daily precipitation is included on the secondary y-axis for the unprocessed (top) and final (bottom) datasets and the number of half-hourly NaNs for this two-month period is included for each step.

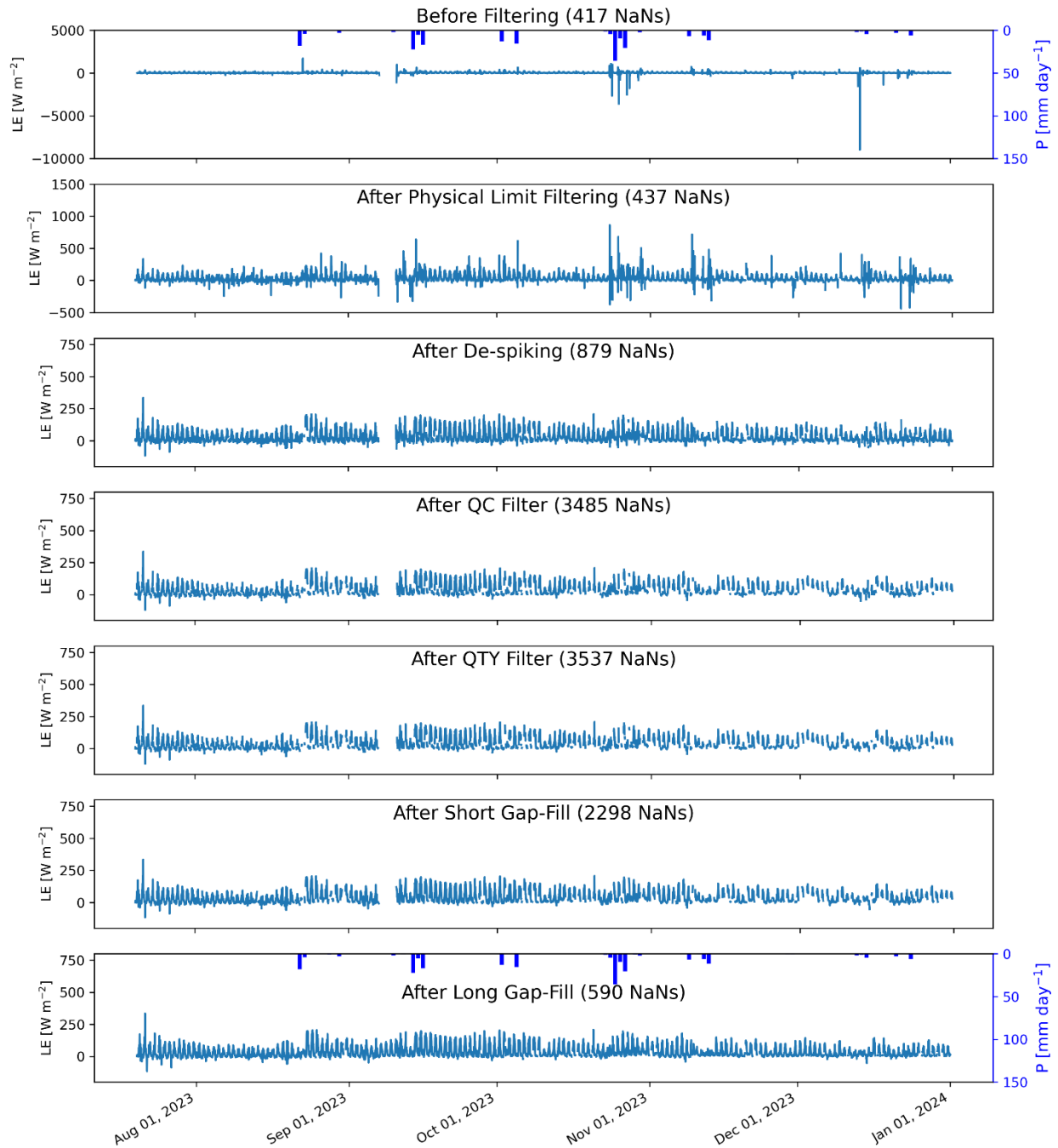


Figure 4.8. Timeseries of LE Data for Nueces at Each QA/QC and Processing Step. Half-hourly LE measurements at the Nueces site (US-EA6) before any processing (top) and after each successive processing step; daily precipitation is included on the secondary y-axis for the unprocessed (top) and final (bottom) datasets and the number of half-hourly NaNs is included for each step.

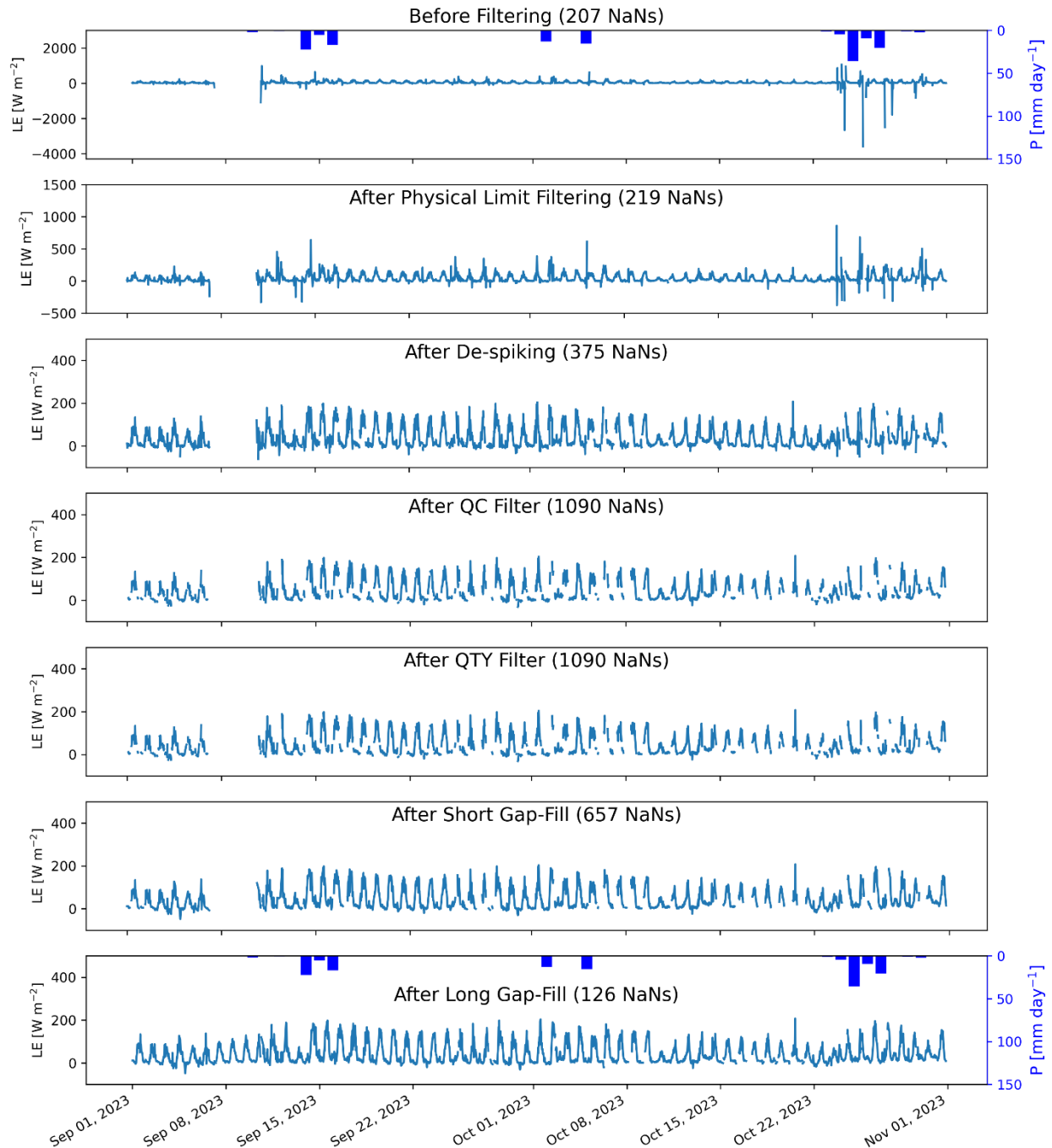


Figure 4.9. Subset of LE Data for Nueces at Each QA/QC and Processing Step. Subset of half-hourly LE measurements at the Nueces site (US-EA6) from September 1 through November 1, 2023, for the unprocessed data (top) and after each processing step, highlighting the gap in data collection in early September 2023 likely due to an obstruction on the infrared gas analyzer; daily precipitation is included on the secondary y-axis for the unprocessed (top) and final (bottom) datasets and the number of half-hourly NaNs for this two-month period is included for each step.

Measurements of LE are directly used to calculate ET (Equation 3.3). The overall effect of the filtering, de-spiking and gap-filling steps applied to the LE datasets is shown through a comparison of cumulative ET throughout the contract period at the Cibolo (US-EA4), Uvalde (US-EA5) and Nueces (US-EA6) sites, calculated from the LE dataset at each progressive step of filtering and processing (Figures 4.10, 4.11 and 4.12, respectively).

The 6-week gap in data collection at the Cibolo site remains, although shorter gaps in October 2022 and January 2023 are filled in during the long gap-fill step (Figure 4.10). Large increases or decreases in ET are seen for the “unprocessed data,” which result from the large (up to $\pm 10,000 \text{ W m}^{-2}$) spikes in LE that existed prior to any processing. The filtering and de-spiking steps led to progressively lower cumulative ET, but the gap-filling techniques brought the cumulative ET back up to nearly exactly the same values as what was originally calculated after the initial processing step of removing LE measurements based on expected limits (Figure 4.10). This is only the case for the Cibolo dataset, and is therefore interpreted to be coincidental.

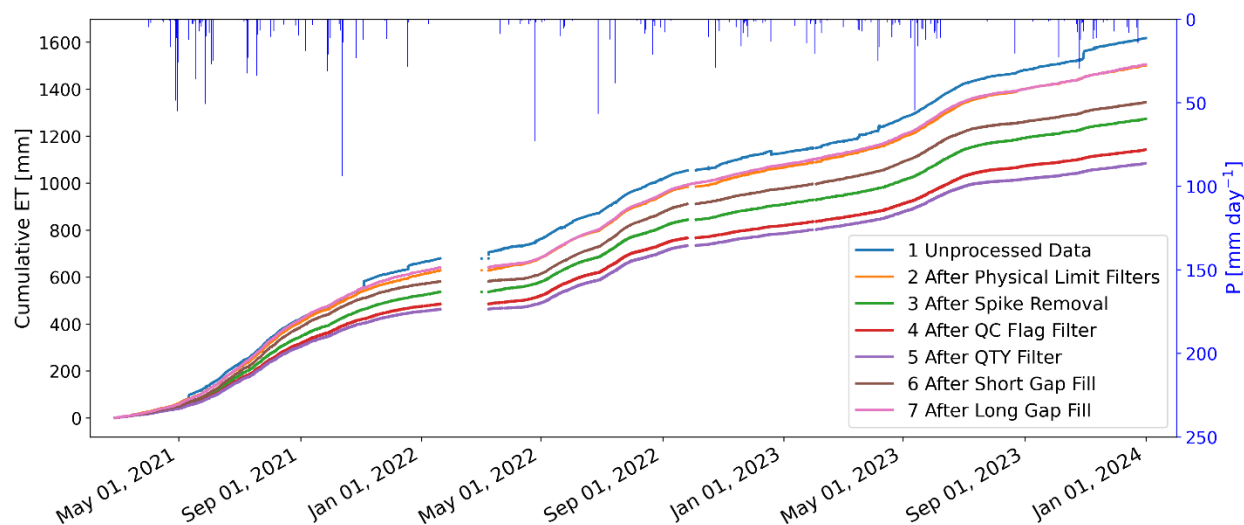


Figure 4.10. Comparison of Cumulative ET at Cibolo After Each QA/QC Processing Step. Cumulative ET at the Cibolo site (US-EA4) over the duration of the contract period calculated for the unprocessed data (blue) and after each processing step; daily precipitation is included on the secondary y-axis.

Cumulative ET calculated after the different processing steps for the Uvalde site followed trends similar to the Cibolo site, with two exceptions. First, the “QTY Filter” step has a minimal effect on the cumulative ET, suggesting that any measurements that would have been removed during this step had already been filtered based on expected limits, spike detection, and/or QC grades. Second, the final cumulative ET values were slightly lower than the ET values calculated after the initial filtering based on expected limits (Figure 4.11).

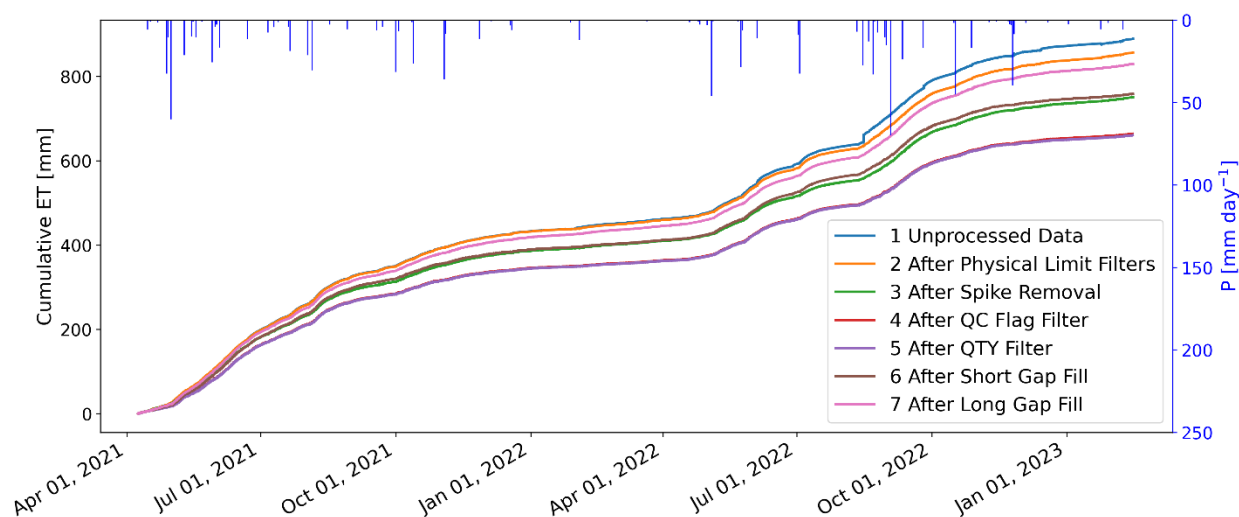


Figure 4.11. Comparison of Cumulative ET at Uvalde After Each QA/QC Processing Step. Cumulative ET at the Uvalde site (US-EA5) over the duration of the contract period calculated for the unprocessed data (blue) and after each processing step; daily precipitation is included on the secondary y-axis.

For data collection at the Nueces site during this contract period, a comparison of cumulative ET calculated after each processing step shows the effect on overall ET as well as the locations of gaps in data and the effectiveness of the gap-filling techniques (Figure 4.12). As of December 31, 2023, the cumulative ET calculated after all processing steps was larger than the “unprocessed data” and the data filtered based on expected limits. This is the result of a series of large negative LE measurements in October 2023 and a single, large, negative spike in LE that occurred in December 2023 (Figure 4.8). Similar to the Uvalde dataset, the “QTY Filter” processing step did not result in a significant change to the cumulative ET calculation at the Nueces site.

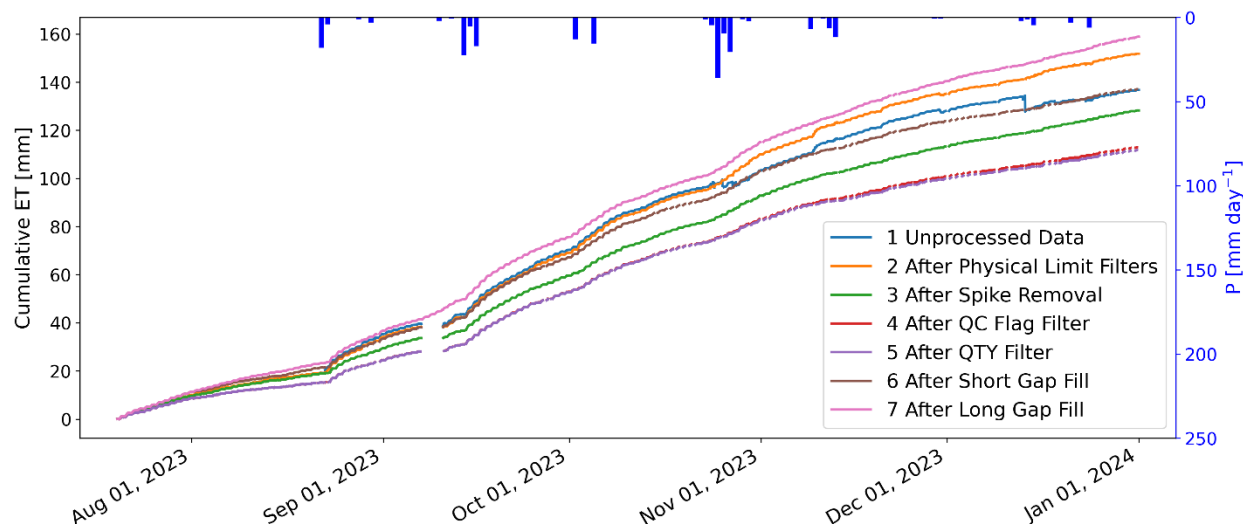


Figure 4.12. Comparison of Cumulative ET at Nueces After Each QA/QC Processing Step. Cumulative ET at the Nueces site (US-EA6) over the duration of the contract period calculated for the unprocessed data (blue) and after each processing step; daily precipitation is included on the secondary y-axis.

4.2 Limitations of Processed Data

The results presented in Section 4.1 highlight the effects of the filtering, de-spiking, and gap-filling techniques used on these datasets. Ultimately, the percentage of missing flux data and the cumulative values of ET generated from the provisionally processed datasets (*Provisional ET Data*) were not drastically different than the values calculated after the initial filtering step based on expected limits of variables. However, when interpreting the final ET datasets, it is important to note that ~40% of LE measurements were discarded based on detection of outliers, poor QC grades and/or the number of 10-Hz measurements in a half-hour interval during the processing of these datasets, the majority of which were filled in using higher-confidence data. In addition, a significant gap in post-processed data still exists for the Cibolo site from January 19 through March 9, 2022, when the station was without power. This gap is too long to fill with conventional techniques, and therefore any subsequent analyses of water budgets that includes this time interval will be impacted.

Finally, we note that an error in the EasyFlux-DL code installed on the CR1000X dataloggers at the Cibolo and Nueces sites was discovered in late 2023. That error erroneously reset the height of canopy variable (“height_canopy”) from the user-defined value (e.g., 8 m at the Cibolo site) to a default value of 0.5 m. The “height_canopy” variable has since been updated in the EasyFlux-DL program installed on the Cibolo site datalogger. The raw, 10-Hz data obtained

from the Cibolo site spanning the date of the station upgrade (January 13, 2023) through December 13, 2023, were reprocessed using the EasyFlux-PC software to compare the effect of an incorrect “height-canopy” measurement on the half-hourly flux values. Due to issues with the storage of 10-Hz data at the Cibolo site, the raw 10-Hz data were only available for reprocessing from January 14 through April 11, 2023, and from July 25 through October 6, 2023. A comparison of the half-hourly flux values generated with the incorrect, default “height_canopy” value and the reprocessed data using the correct “height_canopy” value show nominal differences between the original and corrected flux data (Figures 4.13 and 4.14) of generally 5% or less. These corrections could be used to further process ET data at the Cibolo site from January 13 through December 13, 2023, and at the Nueces site from July 19, 2023 through December 31, 2023 and beyond, until the EasyFlux-DL program at that station is corrected.

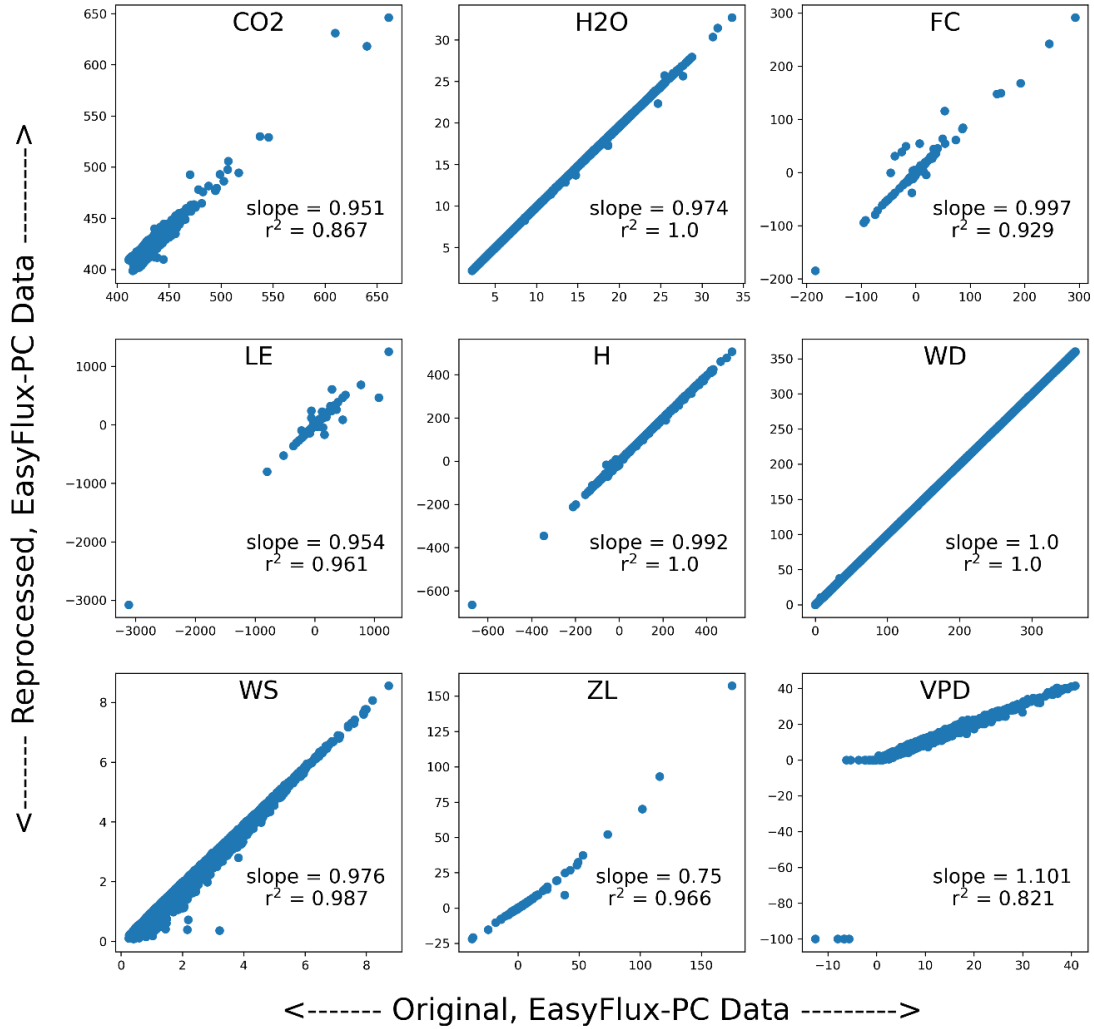


Figure 4.13. Original and Reprocessed Half-Hourly Data at Cibolo from Jan-Apr 2023. Comparison of half-hourly flux values calculated using EasyFlux-DL with the incorrect, default “height_canopy” value (x-axes) and using EasyFlux-PC with the corrected “height_canopy” value (y-axes) at the Cibolo site (US-EA4) from January 14 through April 11, 2023; slope and r^2 values included for each variable; Table 3.1 list units for variables.

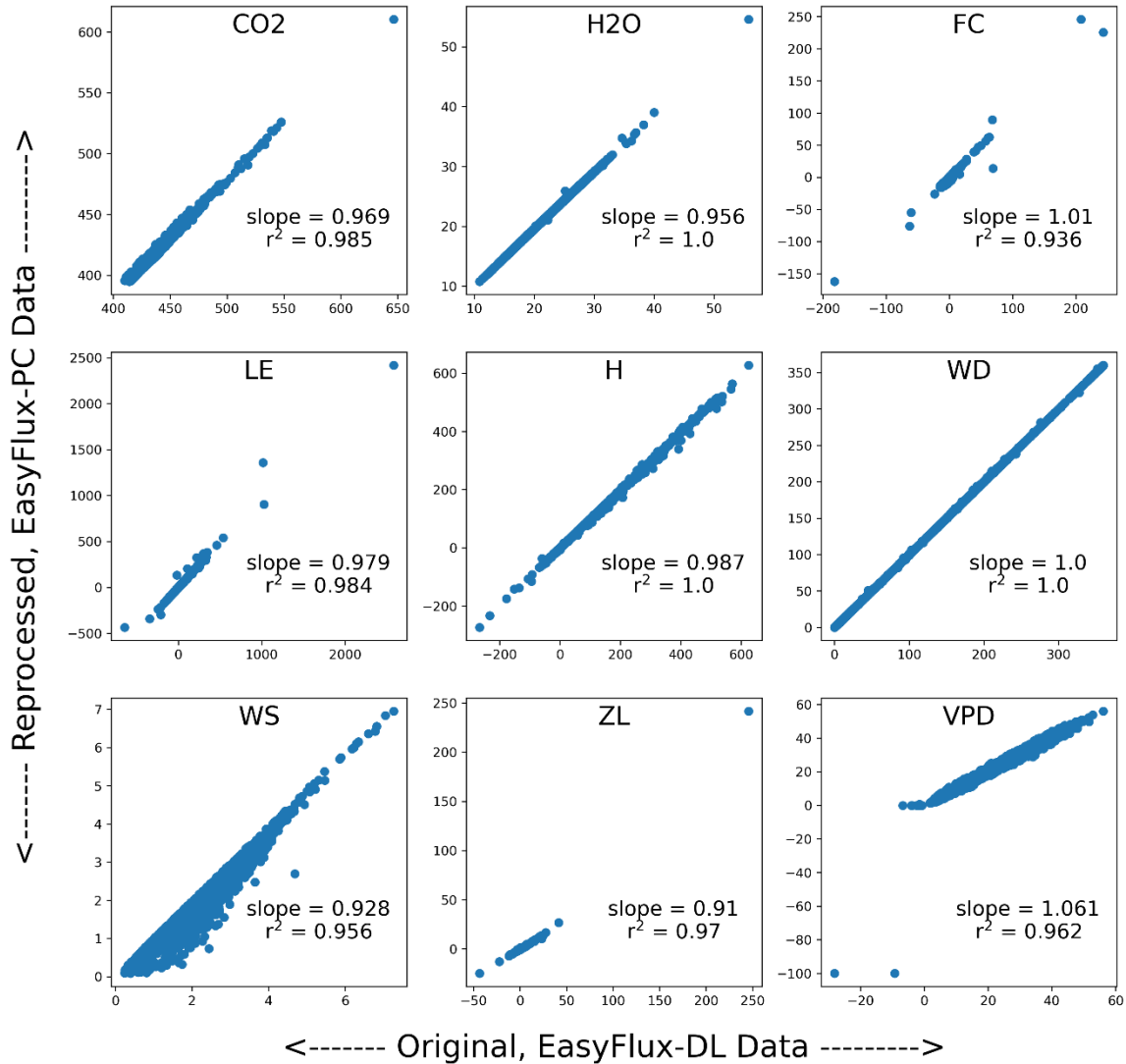


Figure 4.14. Original and Reprocessed Half-Hourly Data at Cibolo from Jul-Oct 2023. Comparison of half-hourly flux values calculated using EasyFlux-DL with the incorrect, default “height_canopy” value (x-axes) and using EasyFlux-PC with the corrected “height_canopy” value (y-axes) at the Cibolo site (US-EA4) from July 25 through October 6, 2023; slope and r² values included for each variable; Table 3.1 list units for variables.

4.3 Preliminary Water Budget Analysis

4.3.1 Cumulative P and ET used in Water Budget Analyses

Cumulative P and ET are presented for all three sites and calculated for “water years” (Table 4.4 and Figures 4.15 through 4.17), defined as the 12-month period beginning on October 1 of a given year and ending on September 30 of the following year ([USGS], 2016). Any given

“water year” is designated by the calendar year in which it ends. Table 4.4 shows the difference in P minus ET (considered to be approximately equal to recharge potential).

Table 4.4. Cumulative P – ET Values Calculated for Water Years [mm]

Water Year	Cibolo (US-EA4)	Uvalde (US-EA5)	Nueces (US-EA6)
2021	109.9	-28.3	N/A
2022	-14.9	84.6	N/A
2023	33.6	39.9	5.4
2024	81.2	N/A	65.4

At the Cibolo site (US-EA4), during water year 2021 (from the date of installation through October 1, 2021), P exceeded ET by 110 mm, indicating at least the potential for recharge. During water year 2022, ET exceeded P by 15 mm, although a 6-week gap in data existed when the station was without power and neither P nor ET was recorded. During water year 2023, P exceeded ET by 34 mm, and through January 1 of water year 2024, P has exceeded ET by 81 mm. During these measurement periods at this site, the results indicate that approximately 19%, 0%, 7%, and 49% of P may be recharging the deeper soil or karst system. What is unclear, however, is the degree of surface runoff that may leave the measurement area or lateral, shallow soil water flow that is neither transpired by plants nor percolating vertically downward and recharging aquifer systems.

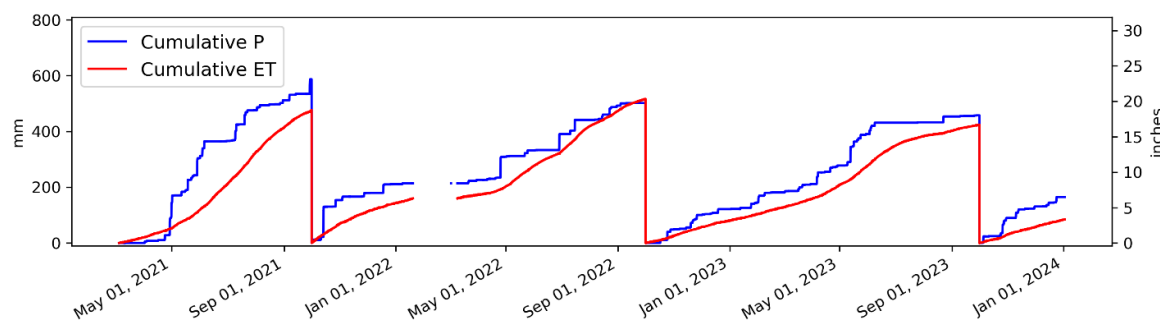


Figure 4.15. Cumulative P and ET at the Cibolo Site. Cumulative P and ET calculated for “water years” at the Cibolo site (US-EA4).

At the Uvalde site, during water year 2021 (from the date of installation through October 1, 2021), ET exceeded P by 28 mm, indicating a deficit (negative recharge) during that time. During water year 2022, P exceeded ET by 84 mm, and during water year 2023 (from November 1 through the decommissioning of the station on March 1, 2023), P exceeded ET by 40 mm. This indicates a potential for recharge in the vicinity of the Uvalde station during water years 2022 and

2023. During these measurement periods at this site, the results indicate that approximately 0%, 16%, and 28% of P may be recharging the deeper soil or karst system.

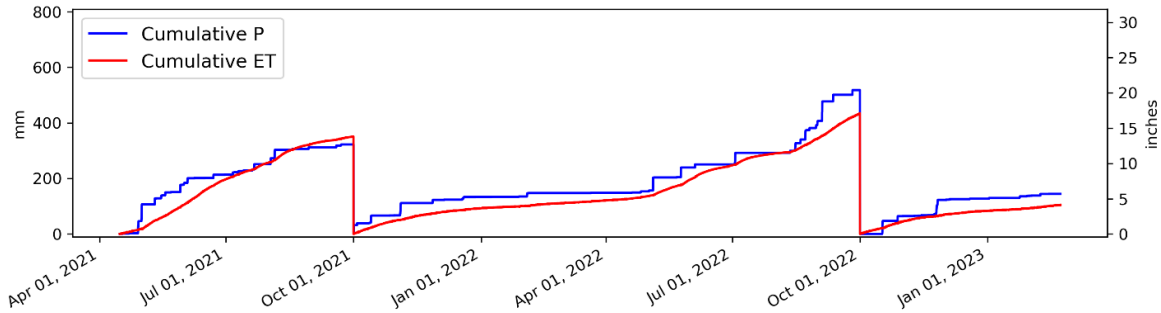


Figure 4.16. Cumulative P and ET at the Uvalde Site. Cumulative P and ET calculated for “water years” at the Uvalde site (US-EA5).

At the Nueces site, during water year 2023 (from the date of installation through October 1, 2023), P exceeded ET by 5 mm, indicating a slight potential for recharge. So far in water year 2024 (from November 1 through January 1, 2024), P has exceeded ET by 65 mm, again indicating a potential for recharge during the wet period.

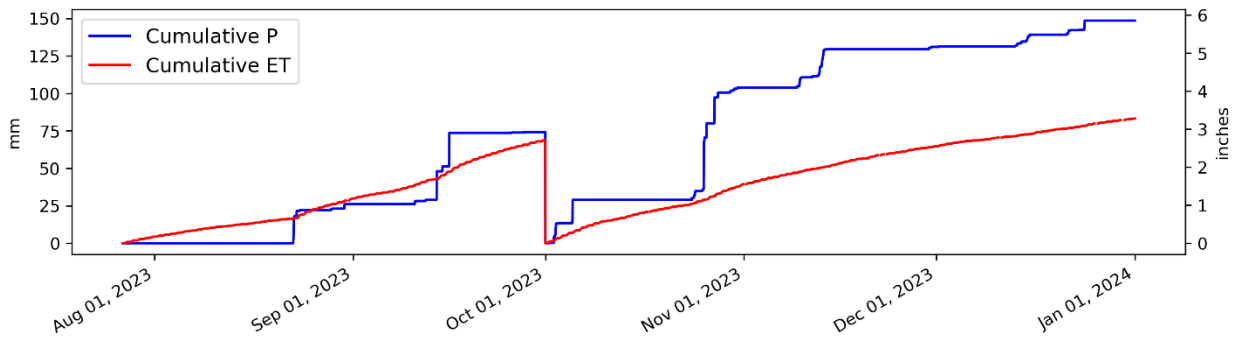


Figure 4.17. Cumulative P and ET at the Nueces Site. Cumulative P and ET calculated for “water years” at the Nueces site (US-EA6).

4.3.2 Monthly P and ET

Monthly values of P, ET and the difference between the two show the potential for recharge on a monthly basis (Figures 4.18 through 4.20 and Tables 4.5 through 4.7). At the Cibolo site, ET consistently exceeded P during the summer months (June through September). However, P generally equaled or exceeded ET during spring, fall and winter (Figure 4.18 and Table 4.5).

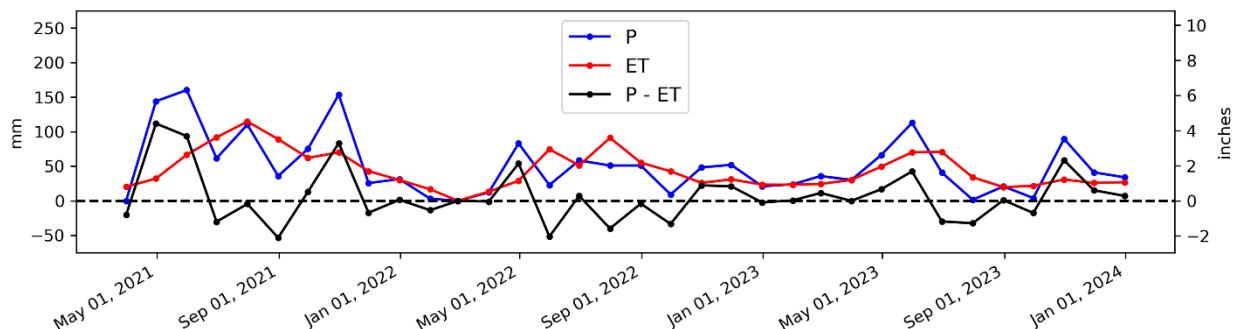


Figure 4.18. Monthly Water Budget at the Cibolo Site. Timeseries of monthly P, ET, and the difference between P and ET at the Cibolo site.

Table 4.5. Monthly Water Budget for Cibolo (US-EA4)

Water Year	Month	P [mm]	ET [mm]	P – ET [mm]
2021	March	0.00	20.4	-20.4
	April	144.0	32.2	111.8
	May	160.3	66.7	93.6
	June	61.5	91.7	-30.2
	July	110.2	114.7	-4.5
	August	35.8	89.3	-53.5
	September	75.2	62.1	13.1
	Total	587.0	477.1	109.9
2022	October	153.7	70.1	83.6
	November	25.7	42.9	-17.2
	December	31.5	30.1	1.4
	January	3.1	16.7	-13.6
	February	0.00	0.00	0.00
	March	12.2	13.3	-1.1
	April	83.1	29.0	54.1
	May	22.9	74.5	-51.6
	June	58.4	51.3	7.1
	July	51.1	91.1	-40.0
	August	51.1	55.2	-4.1
	September	9.1	42.6	-33.5
	Total	501.9	516.8	-14.9
2023	October	48.3	25.9	22.4
	November	52.1	31.0	21.0
	December	21.1	23.4	-2.3
	January	23.9	23.3	0.6
	February	35.8	24.4	11.4
	March	30.2	30.3	-0.1
	April	66.3	49.5	16.8
	May	112.8	70.2	42.6

	June	40.9	70.7	-29.8
	July	1.5	34.0	-32.5
	August	20.8	19.8	1.0
	September	4.1	21.7	-17.6
	Total	457.8	424.2	33.6
2024	October	89.7	30.9	58.8
	November	41.2	25.9	15.3
	December	34.0	26.9	7.1
	Total	164.9	83.7	81.2

At the Uvalde site, ET exceeded P from July through October 2021 and again in July 2022. In general, P equaled or exceeded ET in the winter, spring and fall, resulting in potential recharge during those seasonal periods (Figure 4.19 and Table 4.6).

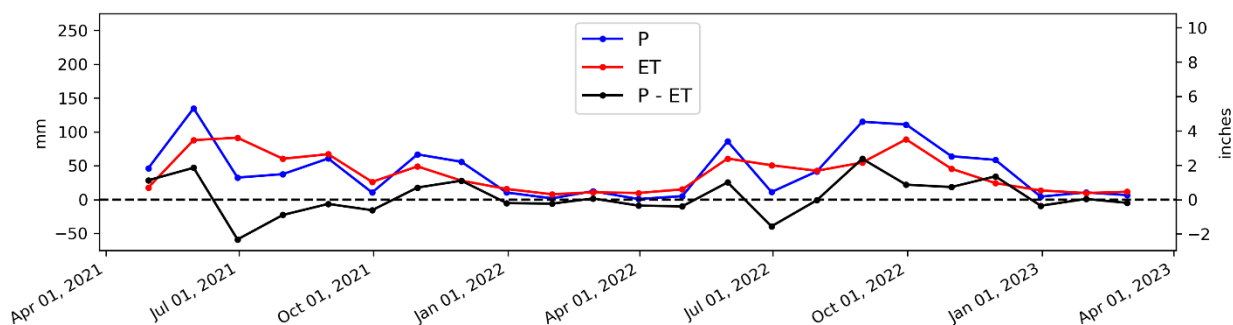


Figure 4.19. Monthly Water Budget at the Uvalde Site. Timeseries of monthly P, ET, and the difference between P and ET at the Uvalde site (US-EA5).

Table 4.6. Monthly Water Budget for Uvalde (US-EA5)

Water Year	Month	P [mm]	ET [mm]	P – ET [mm]
2021	April	46.2	17.7	28.5
	May	134.9	87.9	47.0
	June	32.5	91.5	-59.0
	July	37.6	60.3	-22.7
	August	60.7	67.1	-6.4
	September	10.4	26.1	-15.7
	Total	322.3	350.6	-28.3
2022	October	66.8	49.0	17.8
	November	55.9	28.0	27.9
	December	10.4	15.6	-5.2
	January	1.8	7.8	-6.0
	February	12.5	10.8	1.7
	March	0.8	9.7	-8.9
	April	5.1	15.1	-10.0

	May	86.1	60.7	25.4
	June	11.2	50.7	-39.5
	July	41.7	42.6	-0.9
	August	115.1	54.8	60.3
	September	111.0	89.0	22.0
	Total	518.4	433.8	84.6
2023	October	64.0	45.5	18.5
	November	58.7	24.3	34.4
	December	4.3	13.4	-9.1
	January	10.7	9.7	1.0
	February	6.6	11.5	-4.9
	Total	144.3	104.4	39.9

The Nueces site has not operated long enough to understand the dynamics of P – ET throughout a full water year. Thus far, the results only indicate a potential for recharge during the month of October 2023, when P exceeded ET by 65 mm (Figure 4.20 and Table 4.7).

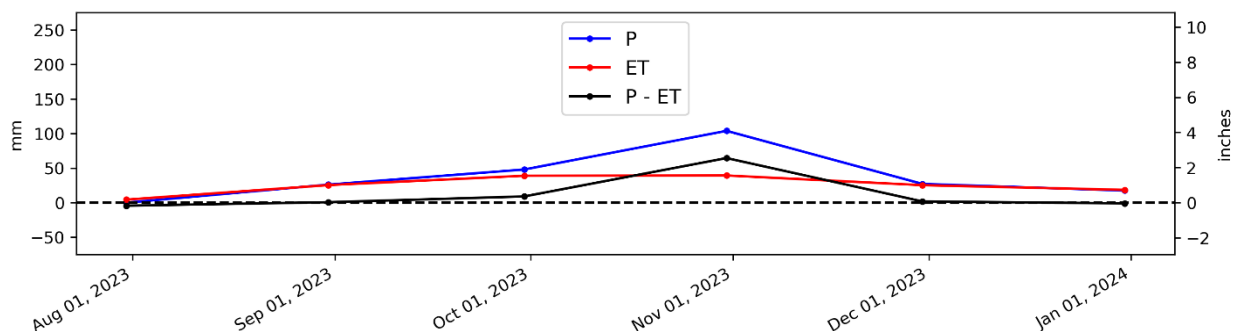


Figure 4.20. Monthly Water Budget at the Nueces Site. Timeseries of monthly P, ET, and the difference between P and ET at the Nueces site (US-EA6).

Table 4.7. Monthly Water Budget for Nueces (US-EA6)

Water Year	Month	P [mm]	ET [mm]	P – ET [mm]
2023	July	0.0	4.4	-4.4
	August	26.2	25.5	0.7
	September	48.0	39.0	9.0
	Total	74.2	68.9	5.3
2024	October	103.9	39.4	64.5
	November	27.2	25.3	1.9
	December	17.5	18.5	-1.0
	Total	148.6	83.2	65.4

At each of the sites being monitored, periods that are dominated by winter rains and leaf-off conditions (resulting in lower transpiration potential) can lead to favorable recharge of shallow

and deeper soil or rock layers. As the length of the dataset increases, and we observe responses of each site to wet periods and drought conditions, we will be able to further understand how interannual variability of meteorological conditions manifest in potential recharge, and whether the deep-rooted plants are extracting water from rock layers, not just from the thin soil layer itself, as was noted by McCormick et al. (2021).

5 Recommendations for Future Work

5.1 Maintenance and Operation

Future work will be focused on maintenance related to the ongoing operation of the Cibolo (US-EA4) and Nueces (US-EA6) stations and standardization of data processing through the AmeriFlux network. Specifically, a new set of ground-based sensors will be installed in soil pit #1 at the Cibolo site to match the upgraded hardware and configuration of the ground-based sensors in soil pit #2 at that site and the two soil pits at the Nueces site (i.e., one each of a CS655 soil water content, temperature and electrical conductivity sensor, a TCAV soil temperature averaging thermocouple, and an HFP01SC self-calibrating heat flux plate) and the EasyFlux-DL program will be updated to reflect the change. Additionally, the EasyFlux-DL program will be updated at both sites when the new version is released, which is anticipated sometime in 2024. Regular maintenance on both stations will occur twice a year moving forward, and will include cleaning of the IRGASON lenses, replacing the IRGA rain wicks, leveling and performing a zero-span on the IRGASON, calibrating the rain gauge, and cleaning and leveling all radiometers. Additional site visits will occur on an as-needed basis to address issues with power, communication, and/or individual sensors.

In addition, we plan to request a site visit from the AmeriFlux Network Technical Team for one or both of the Cibolo and Nueces sites, in which representatives from AmeriFlux will inspect the site, provide feedback on design and implementation, and set up independent eddy covariance sensors to quality control the data collected at our sites. This is anticipated to happen in late 2024.

5.2 Data Processing

The *BEG Filtered Data* product will be submitted to AmeriFlux for all three eddy covariance sites (Cibolo/US-EA4, Uvalde/US-EA5, and Nueces/US-EA6) in early 2024 for AmeriFlux QA/QC to produce the *BASE Product* dataset and for ONEFlux processing to produce the *FLUXNET* dataset, which will be shared with the EAA and considered to be the final dataset. Moving forward, we anticipate processing and sharing the *Provisional ET Data* product with EAA on a quarterly basis, and the *FLUXNET* product on a 6-month or annual basis.

5.3 Water Budget Analyses

This report has presented a preliminary water budget, only considering the difference between P and ET on water-year and monthly bases as a first-order estimate for the potential for recharge, ignoring changes in storage and surface runoff. A model-based approach incorporating these additional parameters, as well as the intensity and duration of precipitation events, is needed to more accurately estimate recharge to the Edwards Aquifer using the ET datasets generated at the eddy covariance sites. To upscale the results, the direct measurements of ET from the eddy covariance stations will need to be correlated to remotely-sensed datasets, such as vegetation indices (e.g., EVI or NDVI) and/or proxies for photosynthesis, such as solar-induced fluorescence (SIF) (Sun et al., 2023), or to model-based regional estimates of ET, such as OpenET (Melton et al., 2022). We anticipate these activities to take advantage of the lengthening dataset being collected at these sites.

References

- Blanken, P., Black, T.A., Yang, P., Neumann, H., Nesic, Z., Staebler, R., Den Hartog, G., Novak, M., and Lee, X. (1997). Energy balance and canopy conductance of a boreal aspen forest: partitioning overstory and understory components. *Journal of Geophysical Research: Atmospheres*, **102**, p. 28915-28927. 10.1029/97JD00193
- Campbell Scientific, Inc. (2018). EasyFlux DL CR3000OP Manual. Logan, UT. Revision 03/2018.
- Campbell Scientific, Inc. (2022). EasyFlux DL CR6OP or CR1KXOP Manual. Logan, UT. Revision 03/2022.
- Chu, H., Christianson, D.S., Cheah, Y.W. et al. (2023). AmeriFlux BASE data pipeline to support network growth and data sharing. *Scientific Data*, **10**, 614. 10.1038/s41597-023-02531-2
- Foken, T., Leuning, R., Oncley, S.R., Mauder, M., and Aubinet, M. (2012). Corrections and data quality control. In M. aubinet, T. Vesala, and D. Papale (Eds.), *Eddy Covariance: A Practical Guide to Measurement and Data Analysis* (p. 85-131). Dordrecht: Springer. 10.1007/978-94-007-2351-1.
- Heilman, J.L., McInnes, K.J., Kjelgaard, J.F., Owens, M.K., and Schwinning, S. (2009). Energy balance and water use in a subtropical karst woodland on the Edwards Plateau, Texas. *Journal of Hydrology*, **373**, 426-435. 10.1016/j.jhydrol.2009.05.007.
- Keese, K.E., Scanlon, B.R. and Reedy, R.C. (2005). Assessing controls on diffuse groundwater recharge using

- unsaturated flow modeling. *Water Resources Research*, **41**, W06010, 12 p. 10.1029/2004WR003841.
- Kukowski, K.R., Schwinning, S. and Schwartz, B.F. (2013). Hydraulic responses to extreme drought conditions in three co-dominant tree species in shallow soil over bedrock. *Oecologia*, **171**, 819-830. 10.1007/s00442-012-2466-x.
- Lasslop, G., Reichstein, M., Papale, D., Richardson, A.D., Arneeth, A., Barr, A., Stoy, P., and Wohlfahrt, G. (2010). Separation of net ecosystem exchange into assimilation and respiration using a light response curve approach: critical issues and global evaluation. *Global Change Biology*, **16**, p. 187-208. 10.1111/j.1365-2486.2009.02041.x
- Lee, X. (1998). On micrometeorological observations of surface-air exchange over tall vegetation. *Agricultural and Forest Methodology*, **91**, p. 39-49.
- Loáiciga, H.A. and Schofield, M. (2020). Climate variability, climate change, and Edwards Aquifer fluxes. Chapter 19 in J.M. Sharp, R.T. Green, G.M. Schindel, eds., *The Edwards Aquifer: The Past, Present and Future of a Vital Water Resource*, *Geological Society of America Memoir*, **215**, Boulder, CO.
- Marclay, R.W. (1995). Geology and hydrology of the Edwards Aquifer in the San Antonio area, Texas, U.S. *U.S. Geological Survey Report*, **95-4186**, 64 p.
- Melton, F.S. et al. (2022). OpenET: Filling a critical data gap in water management for the Western United States. *Journal of the American Water Resources Association*, **58**(6), p. 971-994. 10.1111/1752-1688.12956.
- McCormick, E., et al. (2021). Widespread woody plant use of water stored in bedrock. *Nature*, **597**, p. 225-229. doi:10.1038/s41586-021-03761-3
- McKinney, S.T. (2024). Edwards Aquifer Authority Cibolo (US-EA4), Uvalde (US-EA5), and Nueces (US-EA6) Data (2021-2023). Texas Data Repository Dataverse. <https://doi.org/10.18738/T8/1NSBMG>
- Pastorello, G., et al. (2014). Observational data patterns for time series data quality assessment, paper presented at e-Science, 2014 IEEE 10th International Conference on e-Science. 10.1109/eScience.2014.45
- Pastorello, G., et al. (2020). The FLUXNET2015 dataset and the ONEFlux processing pipeline for eddy covariance data. *Scientific Data*, **7**(1), 225, 27 p. 10.1038/s41597-020-0534-3.
- Reichstein, M. et al. (2005). On the separation of net ecosystem exchange into assimilation and ecosystem respiration: review and improved algorithm. *Global Change Biology*, **11**, p. 1424-1439. 10.1111/j.1365-2486.2005.001002.x.
- Schwartz, B.F., Schwinning, S., Gerard, B., Kukowski, K.R., Stinson, C.L. and Dammeyer, H.C. (2013). Using hydrogeochemical and ecohydrologic responses to understand epikarst processes in semi-arid systems, Edwards Plateau, Texas, USA. *Acta Carsologica*, **42**, 315-325.
- Schwinning, S. (2008). The water relations of two evergreen tree species in a karst savanna. *Oecologia*, **158**, 373-383. 10.1007/s00442-008-1147-2.
- Sharp, J.M., Green, R.T., and Schindel, G.M. (2020). Introduction in J.M. Sharp, R.T. Green, G.M. Schindel, eds., *The Edwards Aquifer: The Past, Present and Future of a Vital Water Resource*, *Geological Society of America Memoir*, **215**, Boulder, CO.
- Sun, A.Y., Bongiovanni, T., Caldwell, T.G. and Young, M.H. (2020). Quantifying diffuse recharge at Camp Bullis, TX: Integrating soil water, evapotranspiration, and remote sensing. *Final Report Submitted to the Edwards Aquifer Authority*, 61 p.
- Sun, Y., Wen, J., Gu, L., Joiner, J., Chang, C.Y., van der Tol, C., Porcar-Castell, A., Magney, T., Wang, L., Hu, L., Rascher, U., Zarco-Tejada, P., Barrett, C.B., Lai, J., Han, J., and Luo, Z. (2023). From remotely-sensed solar-induced chlorophyll fluorescence to ecosystem structure, function, and service: Part II- Harnessing data. *Global Change Biology*, **29**(11), p. 2893-2925.
- Twine, T.E., Kustas, W., Norman, J., Cook, D., Houser, P., Meyers, T., Prueger, J., Starks, P., and Wesley, M. (2000). Correcting eddy-covariance flux underestimates over a grassland. *Agricultural and Forest Methodology*, **103**, p. 279-300.
- Wilcox, B.P. and Huang, Y. (2010). Woody plant encroachment paradox: Rivers rebound as degraded grasslands convert to woodlands. *Geophysical Research Letters*, **37**, L07402. 10.1029/2009g1041929.
- Wilcox, B.P., Owens, M.K., Knight, R.W. and Lyons, R.K. (2005). Do woody plants affect streamflow on semiarid karst rangelands? *Ecological Applications*, **15**, 127-136. 10.1890/04-0664.
- Wilson, K., Goldstein, A., Falge, E., Aubinet, M., Baldocchi, D., Berbigier, P., Bernhofer, C., Ceulemans, R., Dolman, H., and Field, C. (2002). Energy balance closure at FLUXNET sites. *Agricultural and Forest Methodology*, **113**, p. 223-243.
- Wong, C.I. and Banner, J.L. (2010). Response of cave air CO₂ and drip water to brush clearing in central Texas: Implications for recharge and soil CO₂ dynamics. *Journal of Geophysical Research*, **115**, G04018. 10.1029/2010jg001301.

- Wong, C.I., Mahler, B.J., Musgrove, M. and Banner, J.L. (2012). Changes in sources and storage in a karst aquifer during a transition from drought to wet conditions. *Journal of Hydrology*, **468-469**, 159-172. 10.1016/j.jhydrol.2012.08.030.
- [USGS] United States Geological Society (2016). Explanations for the National Water Conditions. Date accessed: 5/24/2022. https://water.usgs.gov/nwc/explain_data.html